DuneFront

Deliverable 10.1

April 2026

DuneFront

Assessing plant traits

Deliverable– D10.1

Deliverable information

Title	Assessing plant traits
Deliverable number	10.1
WP number	10
Author(s)	Malia Scoville (TU-Berlin), Jana Carus, (TU-Berlin), Charlotte Taelman (UGent), Valérie Reijers (UU)
Lead beneficiary	TU-Berlin
Contributors	UU, UGent, TU-Braunschweig
Type	Report
Dissemination level	Public
How to cite	Scoville, M.; Carus, J.; Taelman, C.; Reijers, V. (2026). Assessing plant traits, version 1.0, DuneFront Project Deliverable 10.1. Technische Universität Berlin.
Copyright license*	© Authors and DuneFront consortium, 2024-2027. This work is openly licensed via CC-BY

Versioning and contribution history

Version	Date	Authors (Institution)	Notes
Version 1.0	30.04.2026	Malia Scoville (TU-Berlin), Jana Carus, (TU-Berlin), Charlotte Taelman (UGent), Valérie Reijers (UU)	Final version approved by all Beneficiaries

Funded by the European Union. Views and opinions expressed are however those of the author(s) only and do not necessarily reflect those of the European Union. Neither the European Union nor the granting authority can be held responsible for them.

Funded by the European Union

Cover page

The DuneFront project advances dune–dike hybrid nature-based solutions by integrating ecological processes into coastal protection design. These systems depend on interactions between vegetation and sediment dynamics, with plant functional traits playing a central role in dune formation, stability, and resistance to erosion under wave and storm surge conditions. A mechanistic understanding of these interactions is essential to link ecological functioning with engineering performance.

Work Package 10 contributes by systematically investigating the functional effect and response traits of dune plant species in relation to sedimentation and erosion. Plant characteristics, including stem flexibility, shoot structure, height, and root traits, were linked to erosion and accretion processes using both field measurements and controlled laboratory experiments simulating wind and wave forces.

Our results provide a basis for understanding how vegetation–sediment interactions are governed by plant functional traits and demonstrate their importance for dune stability and resilience under dynamic coastal conditions. This work establishes an empirical foundation for improving process-based models and supports the integration of biodiversity into coastal protection strategies.

DuneFront

Table of Content

List of abbreviations

Abbreviation	Explanation
DEM	Digital Elevation Model
NbS	Nature-based Solution
NDVI	Normalized Difference Vegetation Index
RGB	Red Green Blue
SfM	Structure for Motion
WP	Work Package

1. Introduction

1.1 Overview of work package 10

1.1.1 General objectives

The DuneFront project advances dune–dike hybrid Nature-based Solutions (NbS) by combining ecological processes with engineered infrastructure to enhance coastal protection and resilience. As part of this project, twelve sites across European coastlines have been selected to demonstrate dune-dike hybrid functionality. To realize their full potential as NbS, a deeper knowledge about how the underlying ecological processes function to support dune development and stability is needed. The object of **Work Package 10** is to investigate these functions on several DuneFront demonstrator sites.

The interplay between vegetation and sediment is a foundational process which drives dune development (Bonte et al. 2021; Zarnetske et al. 2012). Coastal plant species affect dune growth with aboveground plant structures trapping windblown sand and belowground plant material stabilizing sediment. These plants have the potential to respond to site specific conditions and stress from wind, waves, or sand burial. These interactions shape plant response and effect traits which can provide insights into understanding of ecosystem functions (Lavorel & Garnier 2002). While conceptually these casual linkages are known, a refined mechanistic understanding with supporting quantifiable data is still needed (McGuirk et al. 2022). Additionally, there remains a lack of plant trait data on a many dune species with particular underrepresentation in belowground trait data despite its known role in sediment stabilization (Ciccarelli & Bona 2022; Freschet et al. 2021).

The intent of this work package is to address these gaps through data collection that include both **above- and belowground trait data** from **multiple species** and to investigate **regional differences** across Europe. Furthermore, to refine our knowledge about **vegetation-sediment interactions** on how coastal species affect dune development, we employ an experimental approach with **wave-flume** and **wind-tunnel** designs. This sand-plant interplay is further supported with **spatial** and **temporal analysis** at two distinct locations.

We quantified key plant traits potentially influencing dune development— such as stem flexibility, shoot organization, plant height and root density and length. These field measurements allow us to establish functional relationships between aboveground and belowground plant traits and their role in sediment capture and stability.

To complement field data, we conducted laboratory experiments in a wave flume and with a portable wind tunnel. Plants rooted in substrate are exposed to aeolian and hydrodynamic forces to create a trait-based sedimentation framework for dune systems.

The trait–erosion–accretion relationships described by the present deliverable will feed into the calibration and parameterization of the vegetation model DuneVeg (now further developed to Living Dunes D10.2). This improved model, together with future expansions to additional species and contexts, will provide reliable forecasts of coupled vegetation–sediment dynamics at multiple spatial scales; its outputs will be upscaled to serve as input for the Predictive Digital Twin (planned DuneFront Key Result KR3.4).

1.1.2 Deliverable tasks

Work package 10 is subdivided into three tasks, two of which are associated with the present deliverable and detailed as follows:

Task 10.1. Assessing plant <u>response traits</u>: quantify growth, expansion and fitness traits of dune-impacting species in the field and link them to recent changes in sediment accretion-erosion (DEM) as delivered by D6.1 (Robin et al. 2025). Results feed Task 10.3 and were coupled back with D6.2-D6.3.

Task 10.2. Assessing plant <u>effect traits</u>: conduct novel lab-, flume, and wind-tunnel experiments to link measurable above and belowground plant traits to sand accretion and erosion potential. Results will be used to calibrate new modules in the medium-scaled erosion-sedimentation models (Task 6.3), following the intermediate calibration of the mechanistic vegetation model (DuneVeg/Living Dunes D10.2).

1.1.3 Report outline

This report summarises the results of these two tasks. To assess and link plant response traits to sediment dynamics (Task 10.1), we employed a multi-method approach with varying spatial and temporal scales. These results are presented in the following two sections. **Section 2** details our evaluation on trait variation of dominant dune species from distinct biogeographical regions. These results support the Living Dunes model calibration addressed in D10.2. In **Section 3**, we present four studies in which remote sensing approaches were applied to investigate vegetation-sediment interactions integrating temporal changes. These studies were mainly carried out at selected sites (Figure 1): Sainte Marie, Soulac and St. Peter Ording (Section 3.1), Oostende (close to Raversijde) (Section 3.2 and 3.3) and St. Peter Ording (Section 3.3). **Section 4** addresses vegetation effects (Task 10.2) on dune erodibility under storm surge conditions as influenced by wave action (Section 4.1) and wind impacts (Section 4.2).

2. Plant response traits

2.1.1 Methods

To measure growth, expansion and fitness traits of dune-impacting species, we collected plant samples from the Atlantic and Mediterranean biogeographic regions with a focus on embryonic and blond dune habitats as described in Deliverable 5.1 (Mordacq & Dahirel 2025). These collections took place in 2025 at three DuneFront demonstrate sites: two locations in France, Sainte Marie la Mer (Perpignan) and Soulac sur Mer in August and in St. Peter Ording, Germany in September (Figure 1). These sites encompass a range in climatic and morpho-dynamic conditions (Castelle & Dahirel 2024, Adeli et al. 2024; Robin et al. 2025) (Table 1). Sainte Marie is characterized by a shallow foreshore with low embryonic dunes and is regularly nourished with sand to counter erosion events. Soulac is highly dynamic with alternating periods of significant sediment accretion and erosion. St. Peter Ording has a wide foreshore allowing for the accumulation and transport of windblown sand resulting in the development of a moderate young but quickly growing dune system. At each location, systematic field measurements were carried out to capture variation in plant functional traits relevant for dune stabilization and sediment dynamics.

Figure 1: Location of the DuneFront demonstrators and the selected sites for plant sampling

For each site, traits were recorded from ten individuals per species, with sampling designed to cover the dominant functional types present in the vegetation community. Measurements focused on species that were either abundant, played a significant ecological role at the site, or occurred across all study sites, ensuring comparability of results. Species were selected from the shortlist in deliverable D4.2, which divided target species in four categorical types based on preexisting knowledge (Dahirel & Bonte 2025). Here we focus on the priority "dune building" species *Ammophila arenaria*, *Elymus farctus* and *Leymus arenarius*. We also investigate species of "conservation importance" namely *Cakile maritima, Artemisia campestris, Calystegia soldanella, Eryngium maritimum, Euphorbia paralias, Medicago marina and Salsola kali*. Additionally, *Carpobrotus edulis* is included from the "introduced" category (Figure 2 & 3).

Table 1: List of site descriptions and sampled species

Site	Species	Site Descriptions
Sainte Marie la Mer, FR	*Ammophila arenaria* *Elymus farctus* *Calystegia soldanella* *Eryngium maritimum* *Euphorbia paralias* *Medicago marina* *Carpobrotus edulis* *Salsola kali*	Shallow foreshore Low embryonic dunes Regularly nourished due to chronic erosion Relative hot-dry climate
Soulac sur Mer, FR	*Ammophila arenaria* *Elymus farctus* *Calystegia soldanella* *Eryngium maritimum* *Euphorbia paralias* *Medicago marina* *Cakile maritima* *Artemisia campestris*	Significant sediment accretion in recent years Relative warm climate
St. Peter Ording, DE	*Ammophila arenaria* *Leymus arenarius* *Elymus farctus*	Relative mild-wet climate White dune reaching 12 meters high Stabilized dune growth

Figure 2: Species sampled include a) Ammophila arenaria, b) Elymus fractus, c) Leymus arenarius, d) Euphorbia paralias, e) Eryngium maritimum, f) Salsola kali, g) Carpobrotus edulis, h) Cakile maritima, i) Medicago marina, j) Artemisia campestris, and k) Calystegia soldanella.

Figure 3: Locations of plant samples from the three sites.

Sample collection

During the field campaign, ten individuals were randomly selected per species at each study site. The selection was carried out in a way that ensured the individuals were representative of the natural occurrence and distribution of the species within the area. For every sampled individual, both aboveground and belowground material was collected. The aboveground biomass was dried for subsequent trait analyses, while the belowground material was preserved in 15% ethanol for later laboratory processing. The procedure followed a standardized set of steps to guarantee consistency across sites and species.

1. **Plot selection**
   A plot measuring 20 × 20 cm² was identified around the selected individual and marked in the field. Care was taken to ensure that the selected plot accurately reflected the typical growth form and density of the species at the site.

2. **Georeferencing**
   The exact location of each plot was recorded using a handheld GPS device (3-300 cm precision, pending conditions), providing precise spatial data for later reference and spatial analyses.

3. **Initial trait measurements**
   Within each plot, plant height and stem density were measured directly in the field. These metrics provided the first quantification of aboveground structural traits.

4. **Photographic documentation**
   Each plot was photographed from both a top-down and a side-profile perspective. Image numbers were systematically recorded in the field notebook to ensure that photographic records could be matched to individual samples at later stages.

5. **Reproductive status**
   Observations were made on the reproductive status of the sampled plants, noting whether seeds, flowers, or other reproductive organs were present. Seeds were collected separately when available, labelled, and stored for later analysis.

6. **Excavation**
   Plants were carefully excavated, with roots extracted to a maximum depth of approximately 30 cm, depending on the species and functional group. Care was taken to minimize root damage during this step.

7. **Root measurements**
   The depth of the root system was measured by recording the distance between the soil surface (bed level) and the point of emergence of the first roots.

8. **Separation of plant material**
   Using shears, the aboveground material was separated from the belowground material in the field. This ensured that the two fractions could be processed and analysed independently.

9. **Preparation of belowground material**
   Roots were gently cleaned of adhering sand and subsequently stored in 15% ethanol. When the root system was too extensive to fit into a single storage bottle, the remaining material was dried and stored in a paper bag for transport and later analysis.

10. **Leaf trait sampling**
    From each aboveground sample, one representative leaf was selected, generally the second leaf from the growth point. This leaf was rehydrated, measured for thickness, and scanned to determine leaf area. Scans were later processed with ImageJ to

calculate total leaf area. These traits formed the basis for specific leaf area and related trait calculations.

11. **Storage of aboveground material**
The selected leaf samples were stored separately from the remaining aboveground biomass to avoid confusion during later analyses. All aboveground material, including the remaining leaves and stems, was dried in paper bags for long-term preservation.

12. **Sample labelling**
All collected materials—aboveground biomass, roots, seeds, and leaves—were labelled according to a standardized scheme: *Site–Species–ID#*. This ensured unambiguous tracking of samples across field and laboratory workflows.

The standardised protocol not only facilitated consistency across sampling sites but also ensured that all relevant plant functional traits could be quantified for subsequent integration into experimental and modelling work.

Laboratory measurements

We performed the following measurements with instruments at the TU-Berlin laboratory upon returning from the field.

1. **Sample drying, weighing and storage**
All samples were stored in labelled paper bags and dried in a drying oven at 60° Celsius for 48 hours. They were then weighed and placed in storage.

2. **Root scans and analysis**
A selection of the preserved roots was prepared and scanned using the EPSON 13000 XL document scanner. The saved images were processed with RhizoVision Explorer to extract root traits data (e.g. root diameter and root length).

3. **Strength tests**
We measured root tensile strength and stem bending strength using a universal testing machine (UniVert). For each plant sample, three roots of similar diameter were collected and scanned prior to tensile strength tests. Roots were clamped on either side and tension was exerted for 20 seconds with 20 mm of displacement. The force at which the root broke was recorded. Similarly, we measured stem strength with a 3-point bending test. Three stems of similar diameter were selected and cut to 6cm in length, measured their diameter and then placed on the support arms of the testing machine. Downward pressure was applied for 20 seconds and across 20 mm displacement and the maximum resistance force of the stem recoded.

Trait measurements

The plant traits as defined below (Table 2) were chosen as they represent distinct features in coastal species that are quantifiable and comparable across species and relate to sedimentation dynamics. Measurements were selected to capture plant functional traits including their response to stress (i.e. burial or desiccation) as well as the effect they have on dune development (i.e. accretion capacity or erosion resistance potential).

Some traits were measured directly in the field such as plant height, stem density and rooting depth. Other traits like biomass, root architecture and strength were measured in the laboratory with the required instruments after the necessary sample processing. Traits were measured according to protocols described by Pérez-Harguindeguy et al. (2013).

The collected dataset provides a representative basis for subsequent analyses of trait–environment relationships and will be integrated into experimental and modelling work in later project stages.

Table 2: List of traits and their functions and measurement descriptions

Trait	Function	Above/below-ground measurement	Unit	Measurement type	Description
Plant Height	Growth Burial resistance	Above	cm	field	Length of plant from point of emergence from sand to tallest leaf/blade gently extended (cm)
Stem Density	Growth Expansion	Above	count	field	Number of stems per 20 cm^2
Root Depth	Growth Nutrient and water acquisition	Above	cm	field	Distance between bed level and first emerging root
Leaf Thickness	Growth Desiccation resistance	Above	mm	lab	Thickness of leaf at midpoint between leaf tip to base measured with a calliper (same leaf used for SLA)
Specific Leaf Area (SLA)	Growth	Above	cm^2/g	lab	Ratio of fresh leaf area to leaf dry mass
Stem Flexibility	Growth Burial resistance	Above	N	lab	Force at stem breaking point as measured by a Universal Testing Machine
Aboveground Biomass	Growth	Above	g	lab	Weight of aboveground material after being dried for 48 hours at 60° C
Belowground Biomass	Growth Anchoring and stabilization	Below	g	lab	Weight of belowground material after being dried for 48 hours at 60° C
Specific Root Length (SRL)	Growth Nutrient and water acquisition	Below	m/g	lab	Ratio of the total root length to root mass

Root Diameter	Nutrient and water acquisition and storage Desiccation resistance	Below	mm	lab	Root diameter as calculated by the RhizoVision Explorer Software
Root Tissue Density (RTD)	Growth Nutrient and water acquisition and storage Desiccation resistance Burial resistance	Below	g/cm^3	lab	Ratio of dry root mass to root volume
Root Surface Area	Growth Nutrient and water acquisition	Below	cm^2	lab	Root surface area as calculated by the RhizoVision Explorer Software
Root/Shoot Ratio	Growth Burial resistance	Above & Below	g/g	lab	Ratio of above- and belowground dry biomass
Root Tensile Strength	Anchoring and stabilization	Below	N	lab	Force at root breaking point as measured by a Universal Testing Machine

2.1.2 Results

Interspecific variation

Above- and belowground traits were grouped and assessed by species. Among the notable interspecific trait variability for **aboveground traits** were (Figure 4), **plant height** showed distinct differences with the grass species (*A. arenaria, E. farctus,* and *L. arenarius*) being the tallest. *C. edulis* showed the highest **total biomass** and *C. soldanella*, the lowest. *A. arenaria* was highly variable in both **plant height** and **total biomass**. **Leaf thickness** was significantly largest in *C. edulis*. **Stem density** was highly variable across all species. Grasses showed the lowest **specific leaf area** compared to non-grasses. **Root-shoot ratio** was highly variable for *E. farctus*. There was a positive correlation between **plant height** and **aboveground biomass** (Figure 5). *E. paralias* had the highest **proportion of aboveground biomass** and *L. arenarius* the lowest (Figure 6).

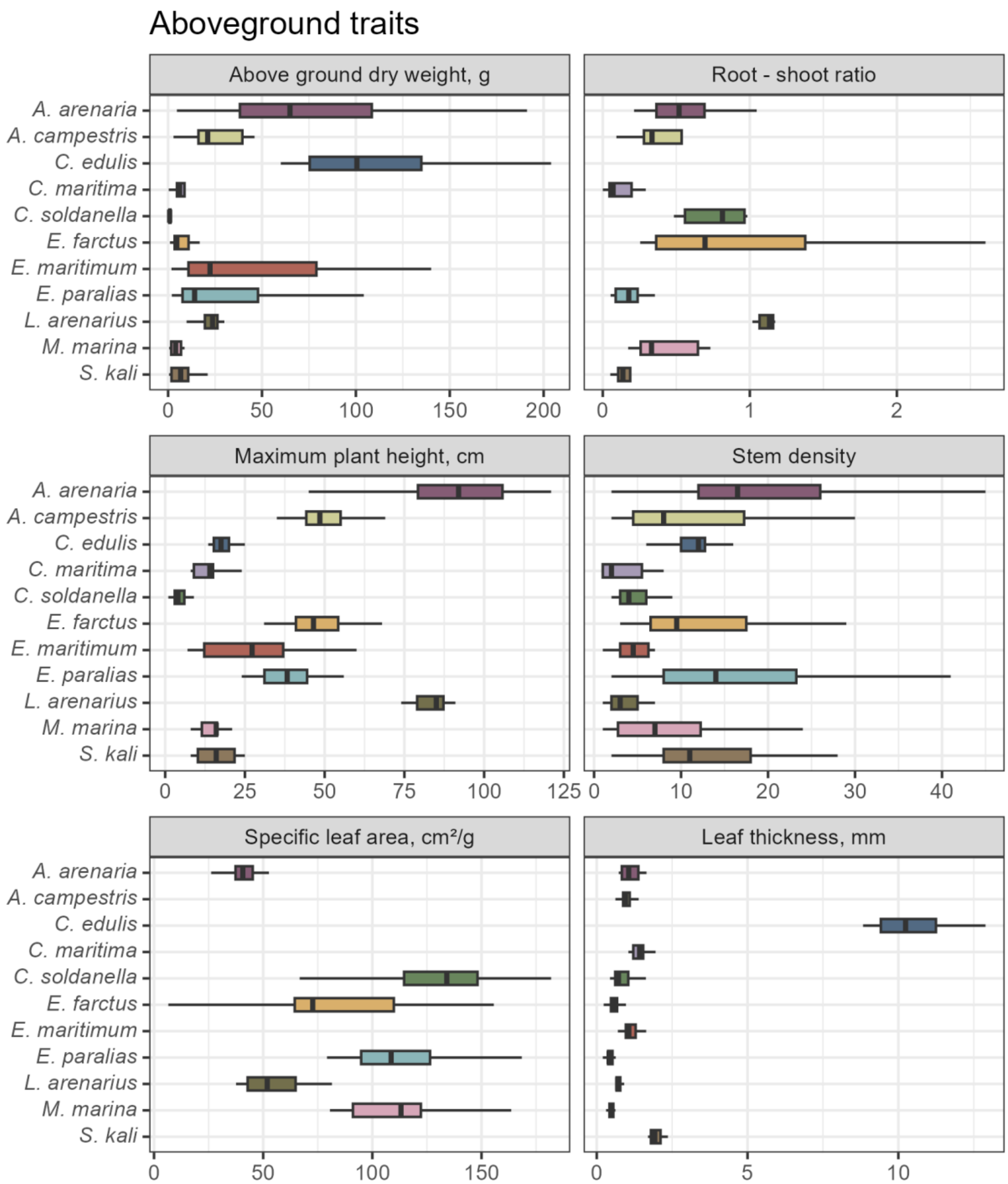

Figure 4: Aboveground plant traits in the 11 species for all three sample sites.

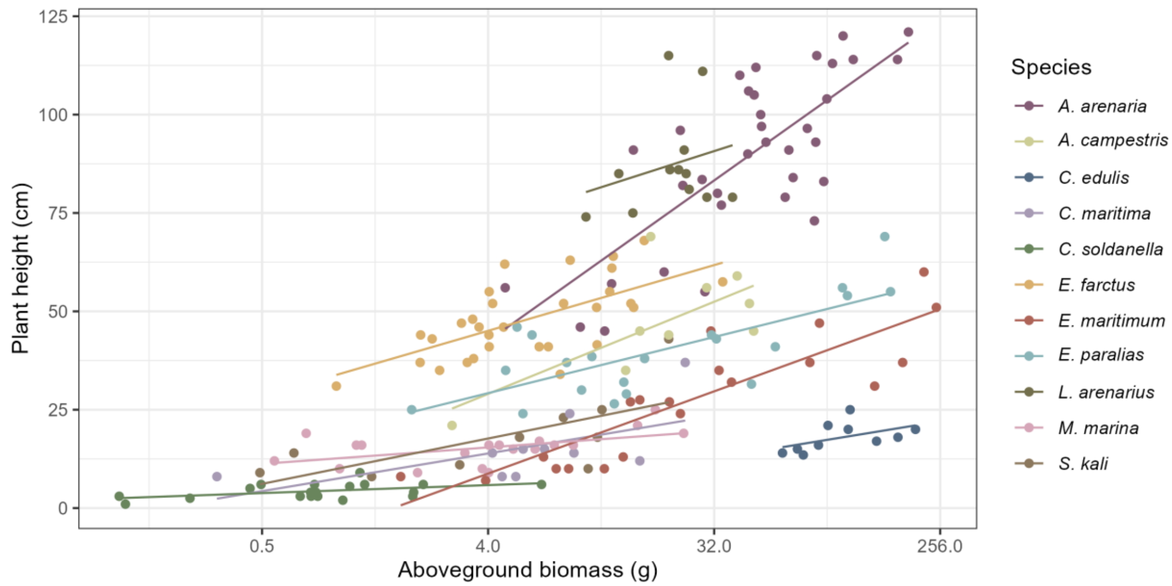

Figure 5: Plant biomass in relation to plant height for all species.

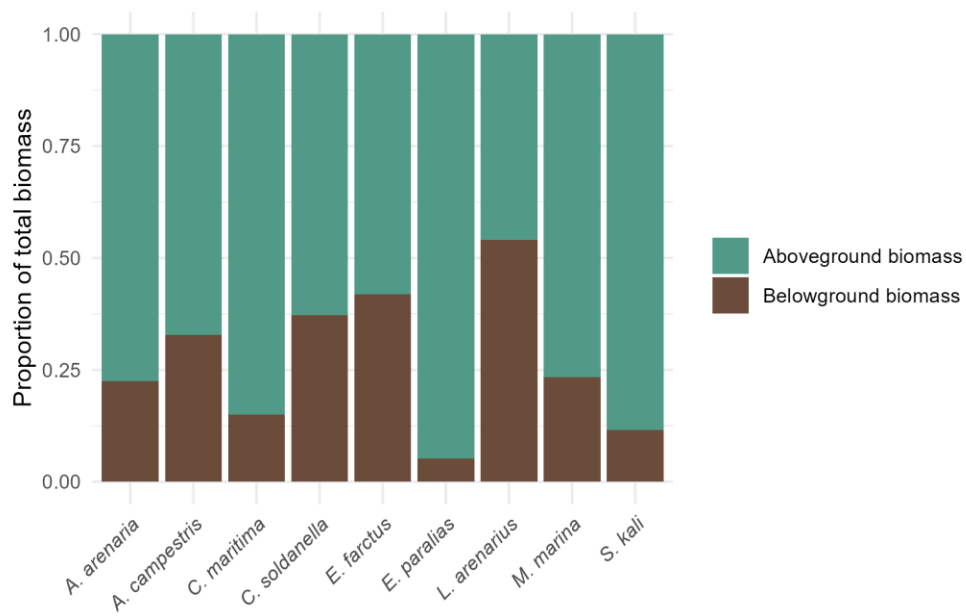

Figure 6: Biomass allocation for all species.

Regarding **belowground traits** (Figure 7), **specific root length** in *A. arenaria, E. farctus*, and *S. kali* had the highest values though were quite variable whereas *A. campestris, C. maritima*, and *M. marina* showed low intra-specific variability. **Root tissue density** was highly variable within species, with the exception of *E. paralias* and *L. arenarius*. The biomechanical properties of roots had strong variability with *S. kali* exhibiting the strongest **root tensile strength.** There was a negative correlation between **tensile strength** and **root diameter** in the three grass species (Figure 8).

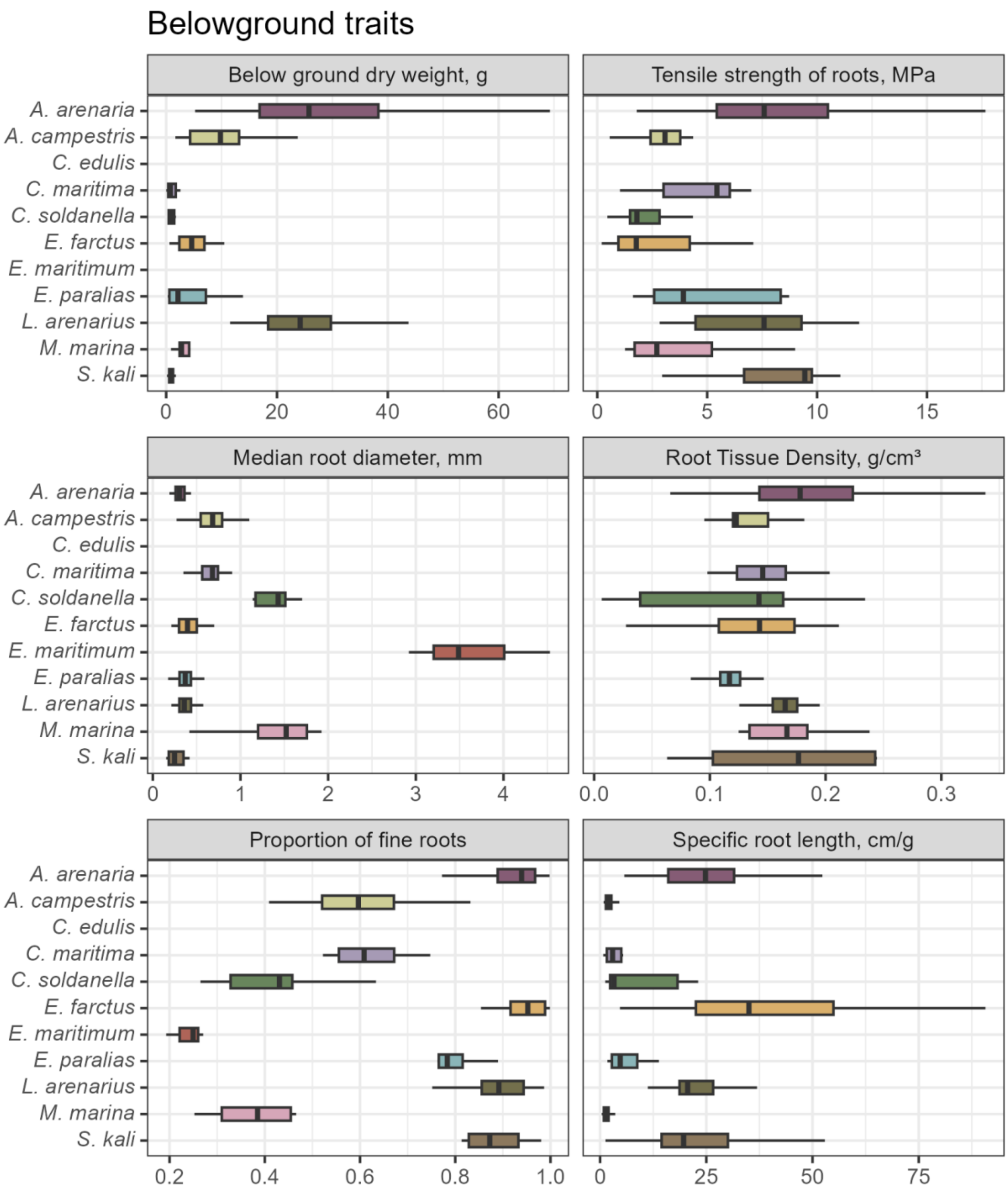

Figure 7: Belowground plant traits in the 11 species for all three sample sites.

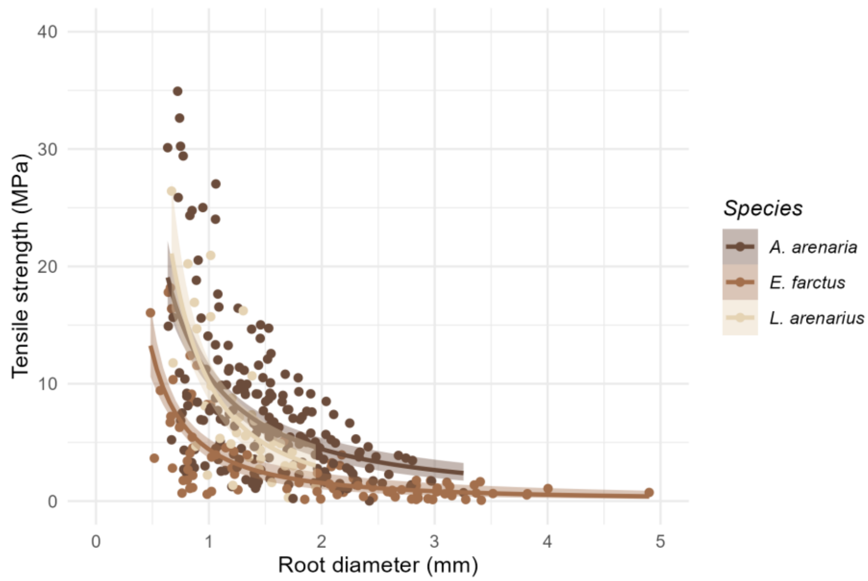

Figure 8: Correlation between tensile strength and root diameter in the three grass species.

Intraspecific variation

In addition to interspecific variability, we observed intraspecific trait variation that differed according to site. Here we illustrate site-specific variability seen in *A. arenaria* and *E. farctus*. We focus on these species as they occurred at all sampling sites and are key dune building species.

For *E. farctus*, several traits differed among sites (Figure 9). The **root–shoot ratio** was significantly higher in St. Peter Ording compared to Soulac and Sainte Marie, with little to now variation in the latter two sites. **Stem density** was highest in Sainte Marie and specific leaf area in St. Peter Ording. **Root tensile strength** was greatest in Soulac, whereas the **proportion of fine roots**, **specific root length**, and **leaf thickness** were lowest in Sainte Marie.

For *A. arenaria*, fewer differences were detected (Figure 10). Sainte Marie differed from the other sites in **maximum plant height**, **proportion of fine roots**, and **specific root length**. **Leaf thickness** was lowest in St. Peter Ording.

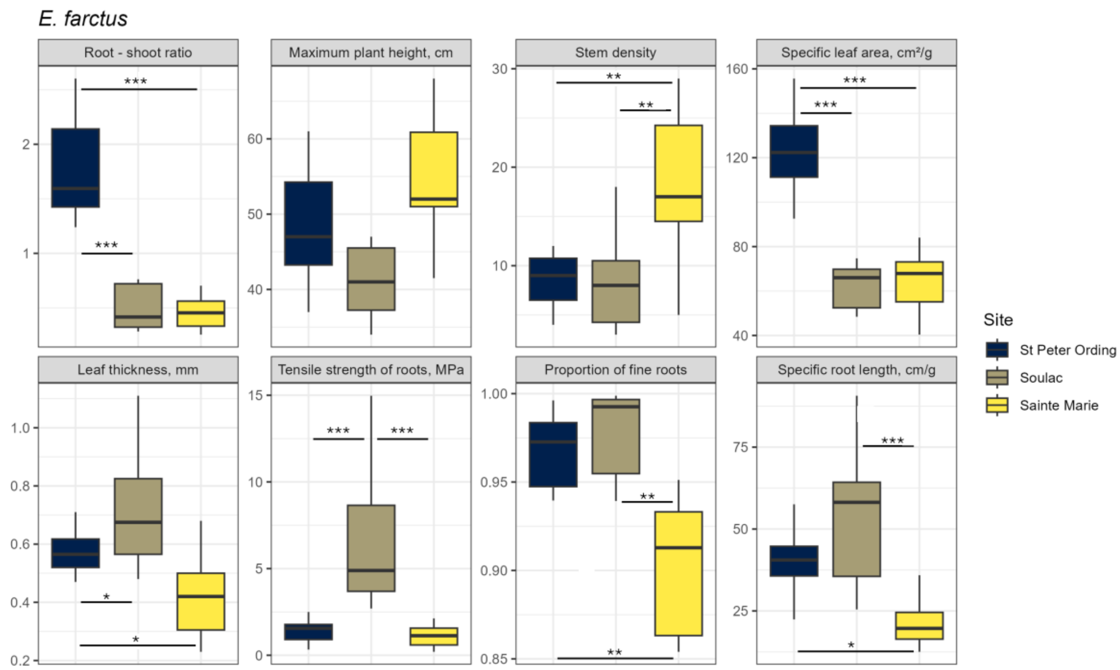

Figure 9: Comparison of the plant traits in E. farctus at all sites. Stars indicate the results of pairwise Wilcoxon rank-sum tests (: p ≤ 0.05 , ** : p ≤ 0.01 , *** : p ≤ 0.001).*

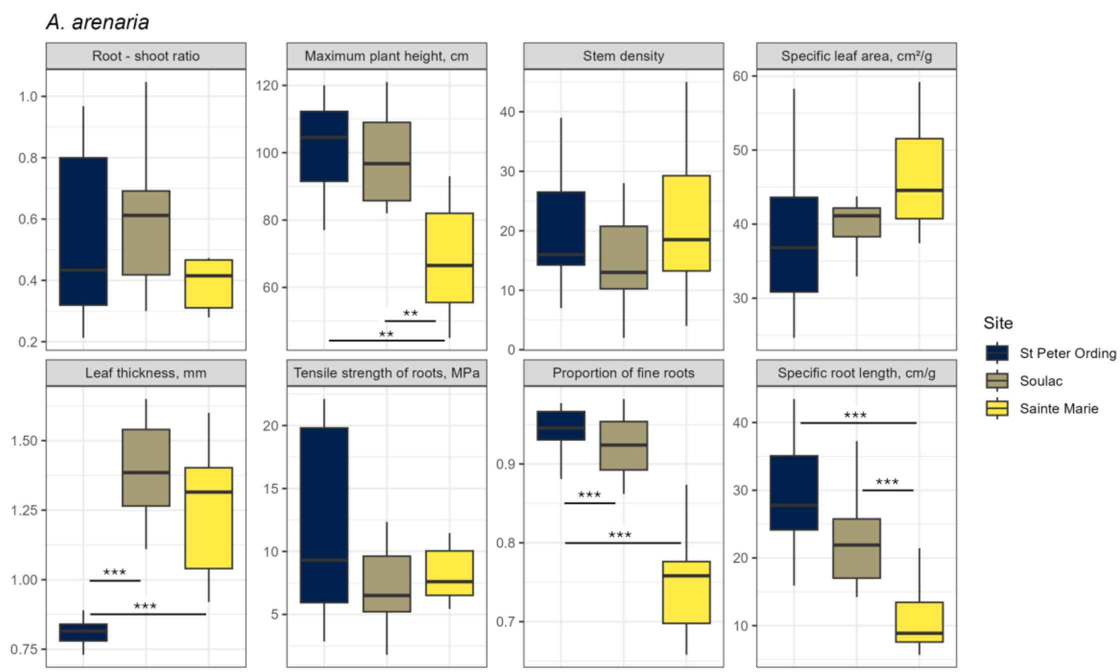

Figure 10: Comparison of the plant traits in A. arenaria at all sites. Stars indicate the results of pairwise Wilcoxon rank-sum tests (: p ≤ 0.05 , ** : p ≤ 0.01 , *** : p ≤ 0.001).*

3. Vegetation-sediment feedback at multiple spatial and temporal scales

3.1 Sediment dynamics and trait variation of several dune plant species

3.1.1 Methods

We investigated trait response to the sedimentation regime using trait information of all species collected at the study sites Sainte Marie la Mer, Soulac and St. Peter Ording (see section 2.1.1 for more information) together with digital elevation (DEM) model data delivered by WP6.1 (Robin et al. 2025). Elevation data for 2022 and 2025 were extracted at points corresponding to the GPS recorded locations for each plant sampled in the field. We used the DEM extracted points to calculate net elevation change for all samples. The species trait data were aggregated (excluding missing values) and classified into three categories accretion, erosion or stable (Table 3) to capture distinct elevation changes in the three-year period. A threshold of ±10 cm was applied to distinguish directional sediment change from background variability, thereby reducing the noise of minor fluctuations while preserving meaningful elevation trends. We then examined how trait expression across all individuals, irrespective of species, varied among different categories of elevation changes.

Table 3: Elevation change categories

Elevation change	Definition
Accretion	More than 10 cm sediment gain
Erosion	More than 10 cm sediment loss
Stable	Less than 10 cm sediment loss/gain

3.1.2 Results

Of the measured traits for all species, the following showed a significant response to sediment dynamics (Figure 11): **Root-shoot ratio** was greater under sediment accretion conditions signifying increased belowground biomass. **Plant height** also increased with positive elevation change. Similarly, **specific root length** and the **proportion of fine roots** increased with sediment accretion indicating plant growth in response to accumulating sediment.

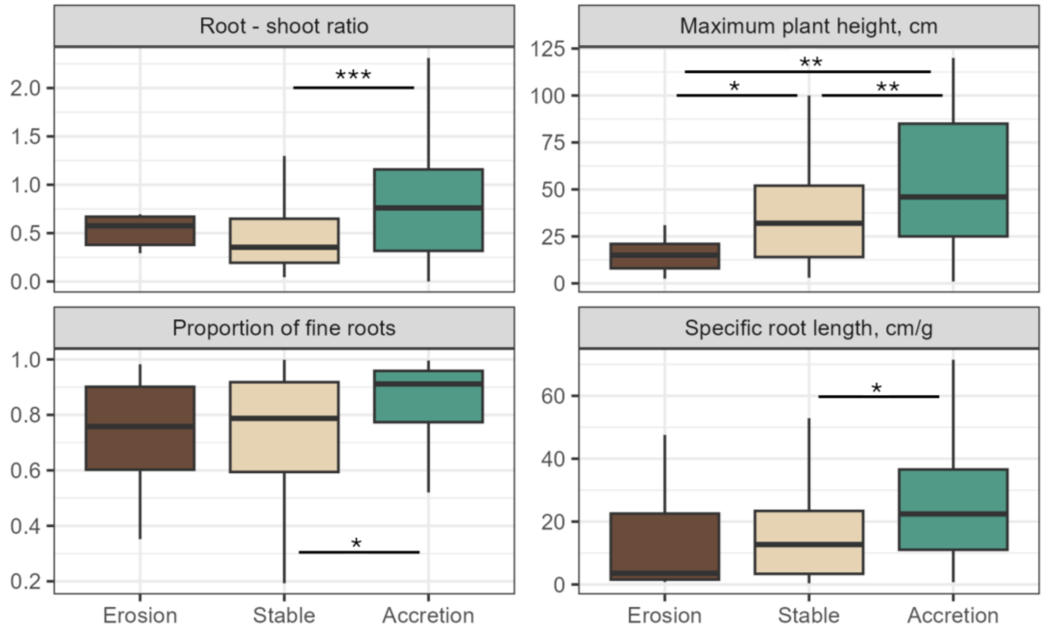

Figure 11: Response of a selected set of traits of all species at all sites to sediment dynamics. Stars indicate the results of pairwise Wilcoxon rank-sum tests (: p ≤ 0.05 , ** : p ≤ 0.01 , *** : p ≤ 0.001).*

3.2 Landscape effect of *A. arenaria* on sand accumulation efficiency throughout the growing season

3.2.1 Methods

We analysed long-term monitoring data of a dune demonstrator site at Oostende, Belgium (close to the Raversijde site, Figure 1). We investigated how the growth of *A. arenaria* impacts the growth and shape of the dune, and at which spatial and temporal scale this engineering species operates within the dune landscape.

Data collection

The dune-for-dike site in Oostende has been rigorously monitored since the start of the marram grass planting in January 2021. The Flemish government (Department Maritime and Coastal Services) has performed near-monthly drone surveys of the dune area, which have rendered high-resolution Digital Elevation Models (2.5 cm, Figure 12 a) and orthophoto mosaics (RGB, 2.5 cm, Figure 12 b) of the entire dune area. Since January 2021, the dune has been measured 32 times.

Data selection

We retrieved the orthophotos of the dune at the start of the growing season (February-March; T2, T14, T22, T28) for every year since the planting. Moreover, we selected the DEMs of the dune area at two different moments in time: at the start of the growing season (February-March; T2, T14, T22, T28) and at the end (September-October; T6, T18, T25, T31), for each year since the start.

Geodata processing

The RGB orthophotos of the dune area were classified using a Support Vector Machine model (SVM-model). This classification model categorized each pixel into either marram grass (1), sand (2) or shade (3), based on the R, G and B values of each pixel. The result of this classification was a raster as an overlay of the dune area, containing 3 classes of pixels. This allowed us to work solely with raster values representing the presence of marram grass (class 1) (Figure 12 c). Finally, to generate a raster representing the cover of marram grass in m^2, marram rasters were multiplied with the area of each pixel (0.025m * 0.025m). Furthermore, elevation rasters from before and after the growing season, were subtracted from each other (autumn minus spring) using DEM differencing, to measure the elevation change of the dune, over the growing season. Finally, 1000 random point locations within the dune were generated (Figure 12 d). At every point, the seasonal elevation change (m) was extracted.

Statistical Modelling

The R package *scalescape (Lowe et al., 2022)* was used to investigate and quantify (1) the marram-sand feedbacks during the growing season, and (2) the spatial scale of effect of marram grass on the landscape. We constructed a linear model with seasonal dune elevation change as the response variable, and marram grass cover at the start of the growing season as the landscape predictor variable. We assumed an exponential spatial weight distribution of *A. arenaria* on the landscape. The model estimated values for both the overall relationship between marram grass cover and the dune elevational changes, as well as the spatial range (m) at which the effect of *A. arenaria* can be observed.

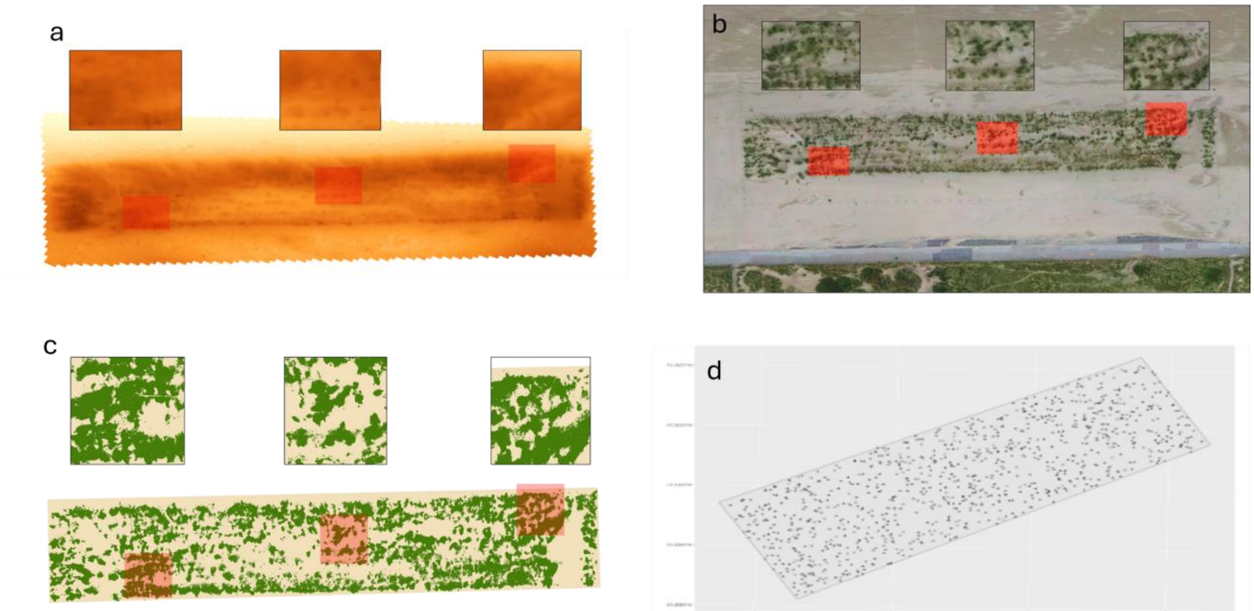

Figure 12: a) Digital Elevation Model of the dune at T26. b) Orthophoto of the demonstrator site, at T26. c) Classified vegetation raster (green is A. arenaria) of the dune at T26. d) 1000 random points within the dune area.

3.2.2 Results

Our results indicate an effect of *A. arenaria* on dune development (Figure 13). Its influence on dune growth was strongest shortly after establishment, became more variable in the following year, and stabilized at moderate positive levels in years three and four.

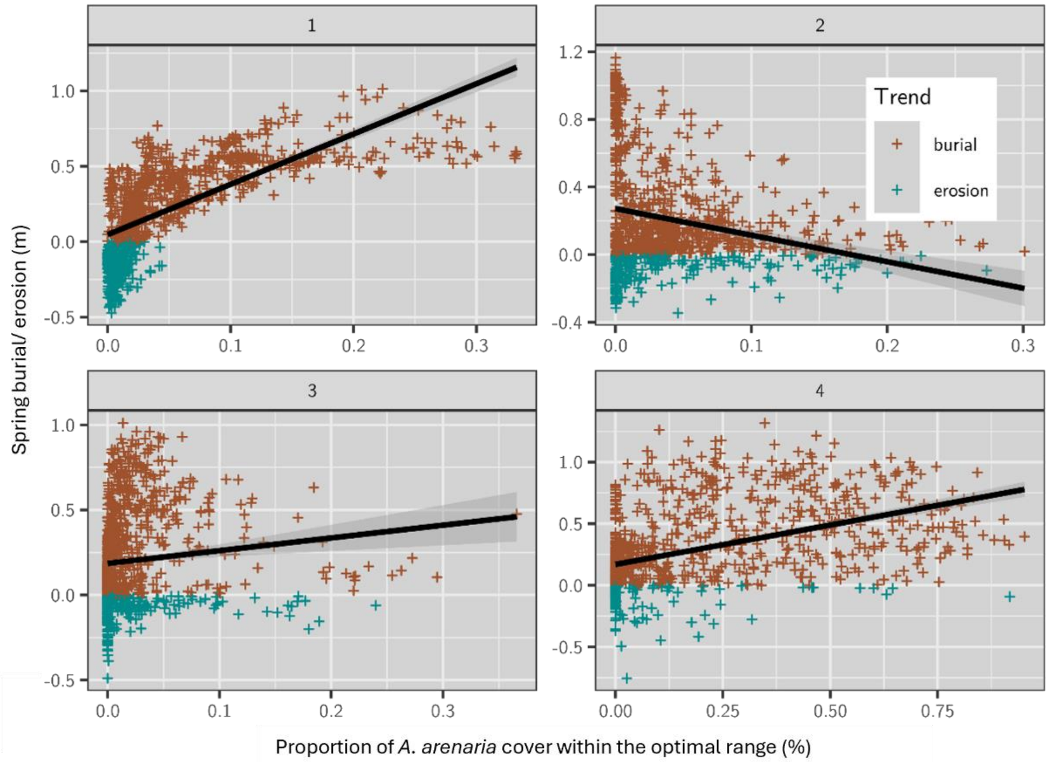

Figure 13: The effect of A. arenaria cover within the optimal range, on the seasonal sand dynamics of the dune, for each year after it was planted. Each panel (years 1–4) relates plant cover within the optimal range to spring elevation change, with points indicating erosion or burial and fitted trend lines.

Overall, the optimal range of *A. arenaria* declined over the four years of our study (Figure 14): The radius at which *A. arenaria* presence influenced burial was reduced by more than eightfold between the first and final year of monitoring.

This pattern suggests a potential link between the spatial scale of influence and vegetation density. When *A. arenaria* is sparse (early stages), individual plants may exert effects over a larger spatial extent, resulting in a broad optimal range. As vegetation becomes denser over time, interactions among plants likely constrain the influence of individual plants or patches, leading to a reduced spatial range of impact.

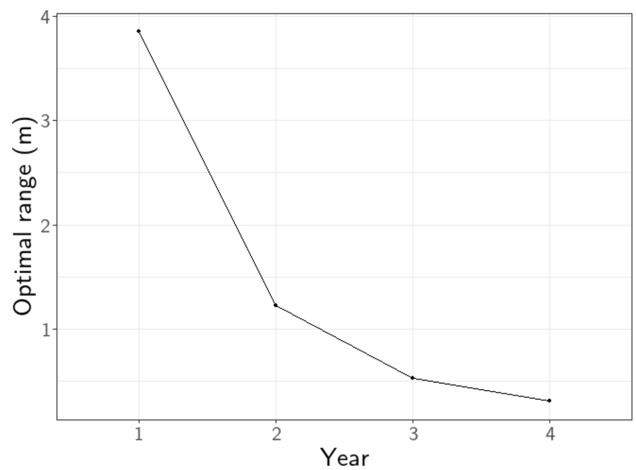

Figure 14: Development of the optimal range of A. arenaria over time.

3.3 Sand accumulation efficiency of several dune plant species

3.3.1 Methods

We investigated the efficiency at which several plant species accumulate volumes of sand during the growing season, thereby either increasing the local dune height, or initiating dune development through the formation of embryonic dunes on the dry beach. Through using a novel technique in the field, we were able to quantify volumes of sand captured by different beach and dune plants on the Flemish coast.

Timing and location

We collected samples along a transect from Oostende (central coast) to De Panne (west coast, close to French border), including the two Belgium demonstrator sites. Samples were taken on the dry beach (the area between the dune toe and the springtide water line) between 2023 and 2025, starting from late spring (May) until the end of the growing season (September).

Data collection

We searched for locations in the dune demonstrator sites or on the dry beach where *A. arenaria*, *E. farctus*, *C. maritima,* or *S. kali* were present. We selected an area (maximally 5 by 5 metres) around each plant and considered this a plot, which was given a unique ID in the field. Each plot was measured for the amount of sand captured by the vegetation. By using the LiDAR sensor on an iPhone 12 Pro, we were able to make a 3D-image of each plot with the app “3D Scanner”. As a result, point clouds were generated of each plot, together with a scaled floorplan (RGB photomosaic from above).

Geodata processing

Point clouds of the dune plots were exported to our laptops and manually processed in CloudCompare. Clouds were cleaned and cropped in order to remove all sources of noise by the surrounding area. Large point clouds consisting of multiple embryo dunes and/or species, were split into mono-species point clouds as much as possible. Point clouds were re-oriented using PCA and were projected towards the origin. We then calculated the surface, volume and maximum height of the point clouds using the 2.5D Volume tool (Figure 15, right).

Image analysis

The floorplans of each plot were processed using Fiji (ImageJ) (Figure 15, left). First, the scales on the photos were used as a measuring reference (m). Then, the outline of the vegetation was manually indicated by drawing one or multiple polygons, using a Wacom tablet. The total vegetation cover in the plot was calculated as the surfaces of all polygons combined.

Statistical modelling

Using the sand volumes, surfaces and species-specific vegetation cover, we performed a linear model through the origin for each species separately, using square-root of plant cover as a predictor variable, and the captured volume of sand per m² as a response. Linear models estimated the strength (efficiency) at which each species captured sand.

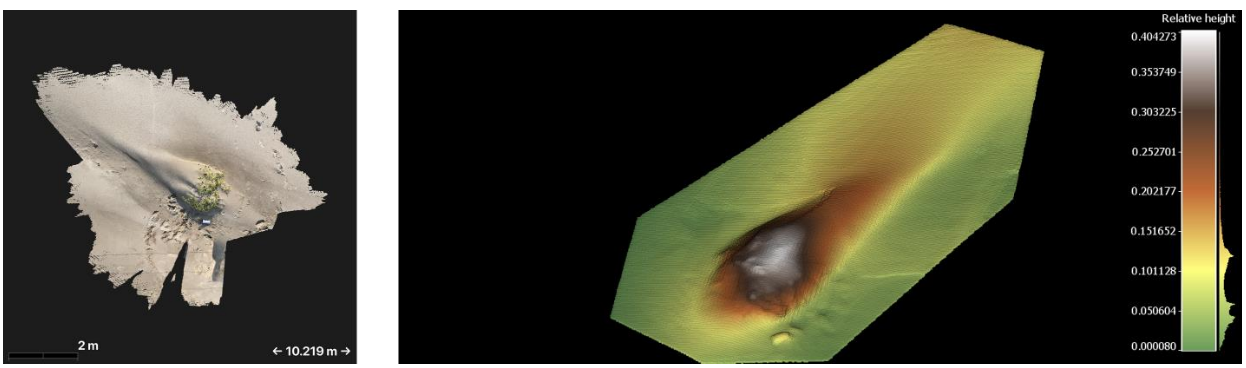

Figure 15: Floorplan of a Cakile maritima embryo dune (left) and point cloud of a dune formed by Cakile maritima (right). The legend indicates the relative height of the dune.

3.3.2 Results

Plant cover had a consistently positive effect on sediment accumulation across all four species (Figure 16). The regression coefficients were comparable among species, with values of 0.12 for *S. kali*, 0.14 for *A. arenaria*, and 0.16 for both *C. maritima* and *E. farctus*.

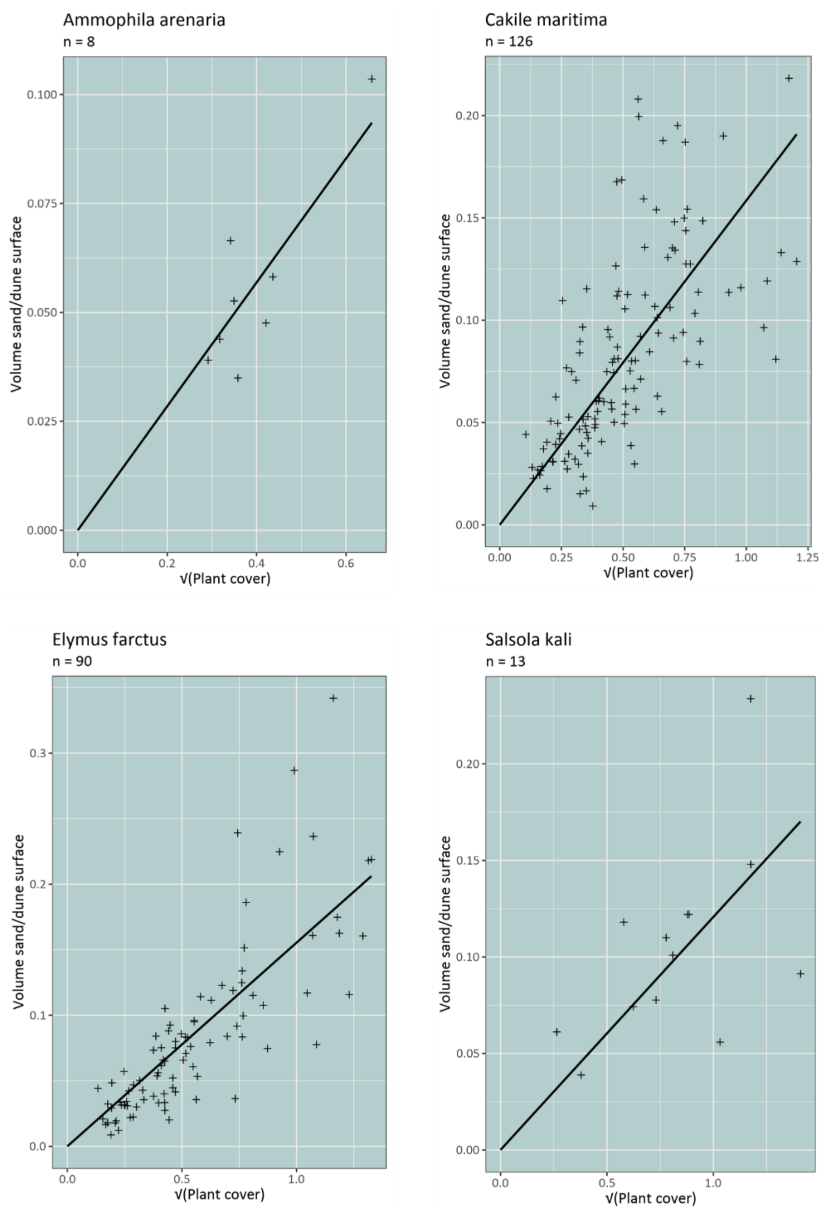

Figure 16: Effect of plant cover on sediment accumulation across four dune-building species.

3.4 Linking plant functional traits with dune dynamics

3.4.1 Methods

Timing and location

In the demonstrator site St. Peter Ording, we followed a multi-scale approach combining vegetation surveys, temporal monitoring, and remote sensing techniques to link plant functional traits with dune morphology and dynamics.

To assess inter- and intraspecific variation in plant trait distributions, vegetation surveys were conducted along nine transects. Along each transect, four plots were established in the different stress zones of the dune i.e. at the toe, face, crest and back of the dune - resulting in 36 sampling plots (Figure 17). Field data were collected in 2025 at four eight-week intervals during the growing season between March and September to capture seasonal variation in vegetation traits and vegetation–sedimentation interactions.

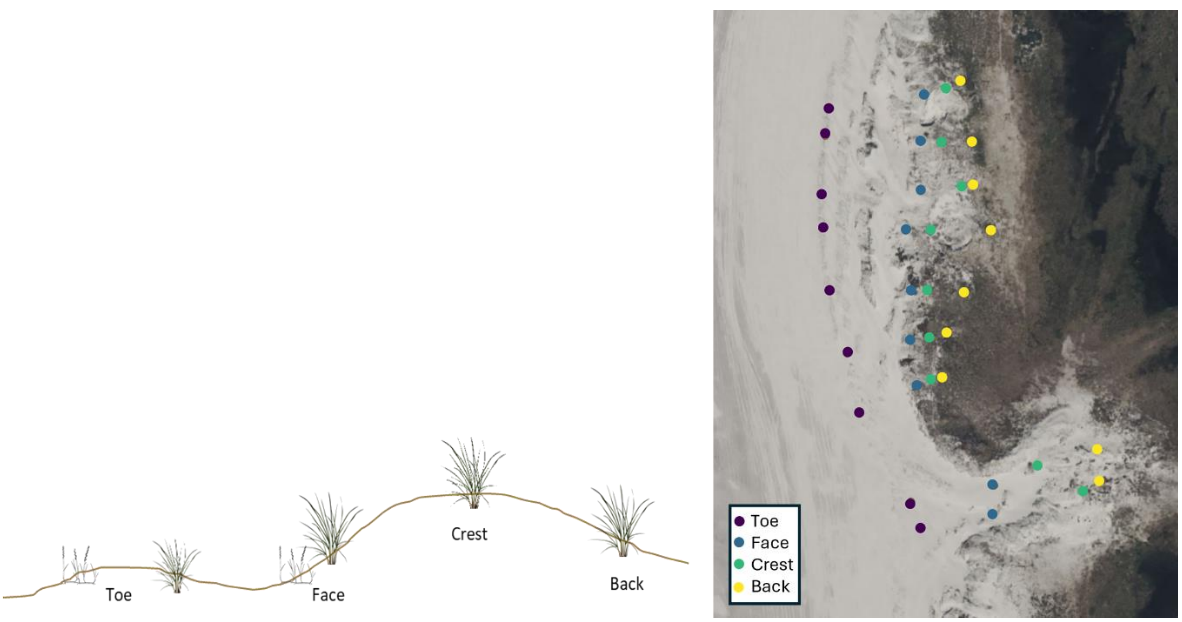

Figure 17: Schematic cross-section of a transect showing the four stress zones (left) and top view of all plots in the study area.

Data collection

Plant traits relevant to stress tolerance, growth strategies, and sedimentation interactions were recorded directly in the field at all sampling campaigns. In September 2025, we additionally collected one individual of the dominant species in each plot and measured maximum plant height, stem density, stem diameter in the field and other parameters like above and below ground biomass and specific leaf area as well as all root parameters in the laboratory (for more detailed information on trait measurements see chapter 2.1.1).

Unmanned Aerial Vehicle (UAV) surveys were employed to capture vegetation and dune morphological changes at fine spatial and temporal scales. A DJI Mavic 3 Multispectral drone was deployed to collect multispectral imagery, including NDVI data. These datasets were processed to derive vegetation indices and map fine-scale spatial patterns of vegetation growth and sand movement (Figure 18).

Trait and remote sensing data was integrated to analyse spatial and temporal relationships between vegetation dynamics and dune morphology.

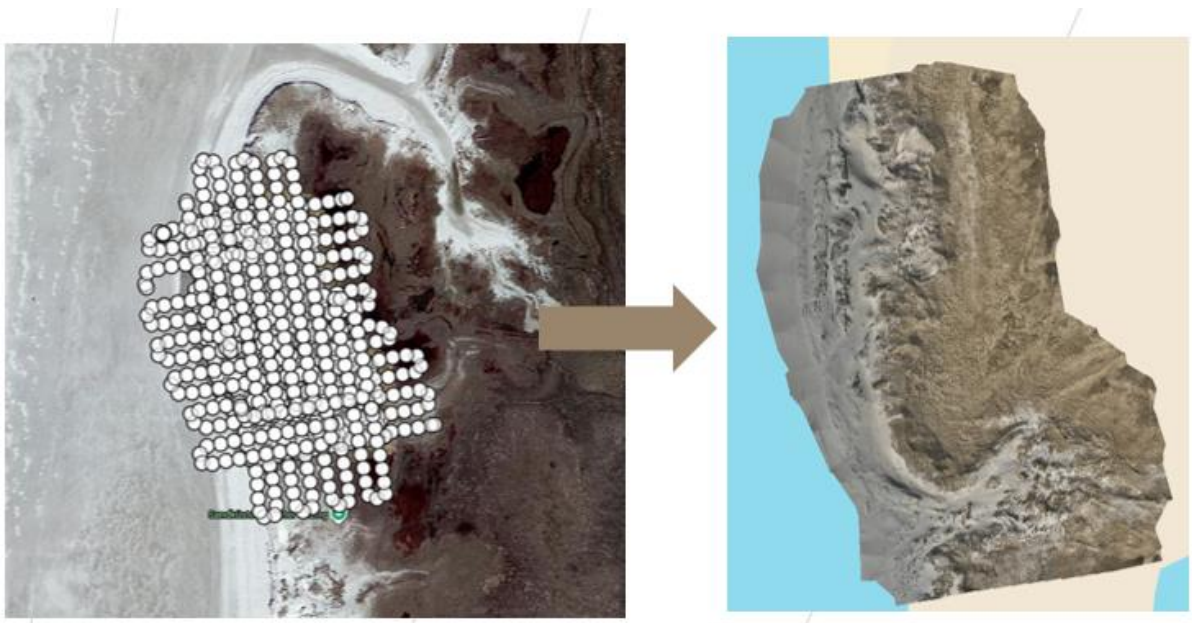

Figure 18: Top view of the study area showing the locations of more than 1,000 individual images acquired during an oblique flight mission (left) and the resulting orthophoto (right).

3.4.2 Results

In the three years preceding our field campaign (2022 –2025), mean dune height increased by an average of 0.53 m yr^{-1}, with increases observed consistently across all four zones (Toe, Face, Crest, and Back). During the 2025 growing season, however, sedimentation was significantly greater at the dune toe, whereas slight erosion occurred at the crest and back of the dune (Figure 19).

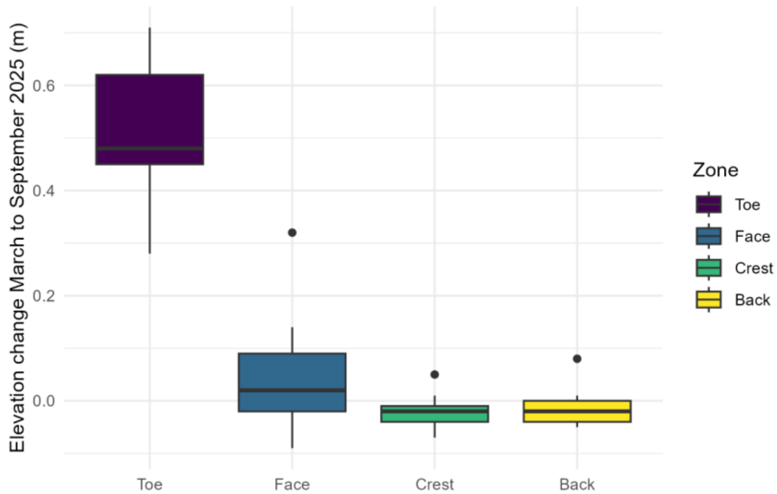

Figure 19: Elevation change from March to September 2025 at the four stress zones.

Combining all species information, several assessed plant traits varied systematically across the defined stress zones (Figure 20). The **root–shoot ratio** was highest at the dune toe and declined toward the inner dune, whereas **aboveground dry mass** and **maximum plant height** increased along this gradient. Both **stem stability metrics** (bending modulus and flexural rigidity) were significantly lower in the toe-zone than in the other locations. A similar pattern was observed for **root tensile strength** and **root tissue density**, both of which were lowest at the dune toe and did not significantly differ between the other plots. No significant differences were observed in the **proportion of fine roots** and the **specific root length**.

Direct trait responses to elevation change were comparatively weak. Only **root tensile strength** showed a response to elevation changes occurring during the growing season (Figure 21), declining with increasing elevation change.

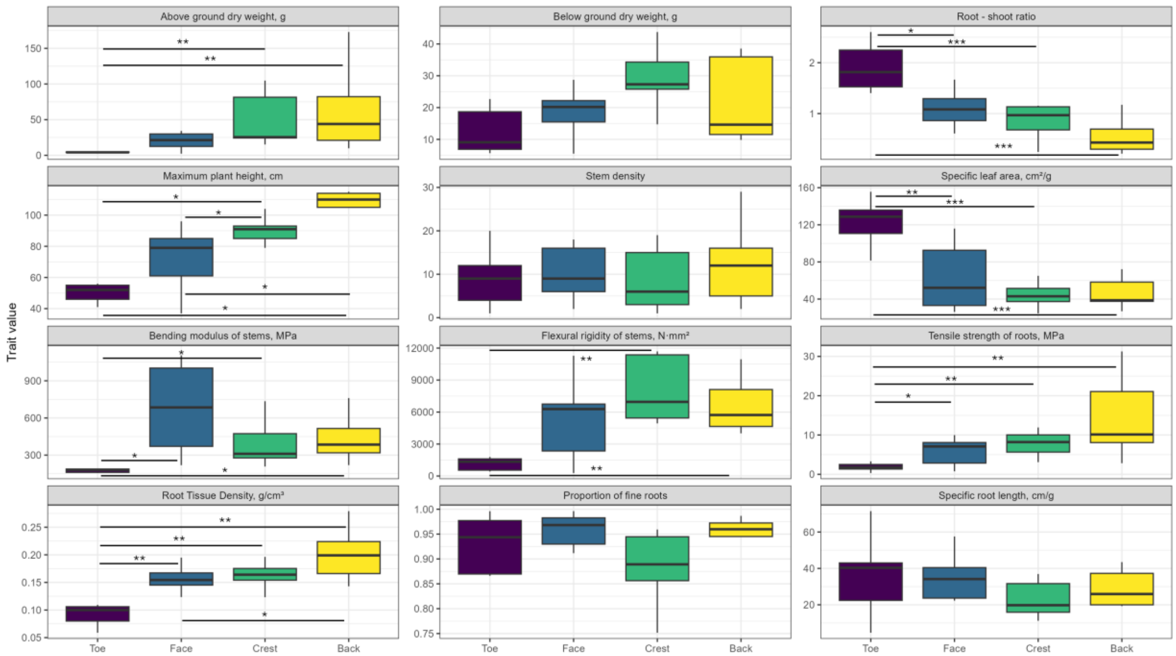

Figure 20: Plant traits of A. arenaria, E. farctus and L. arenarius at each stress zone. Stars indicate the results of pairwise Wilcoxon rank-sum tests (: p ≤ 0.05 , ** : p ≤ 0.01 , *** : p ≤ 0.001).*

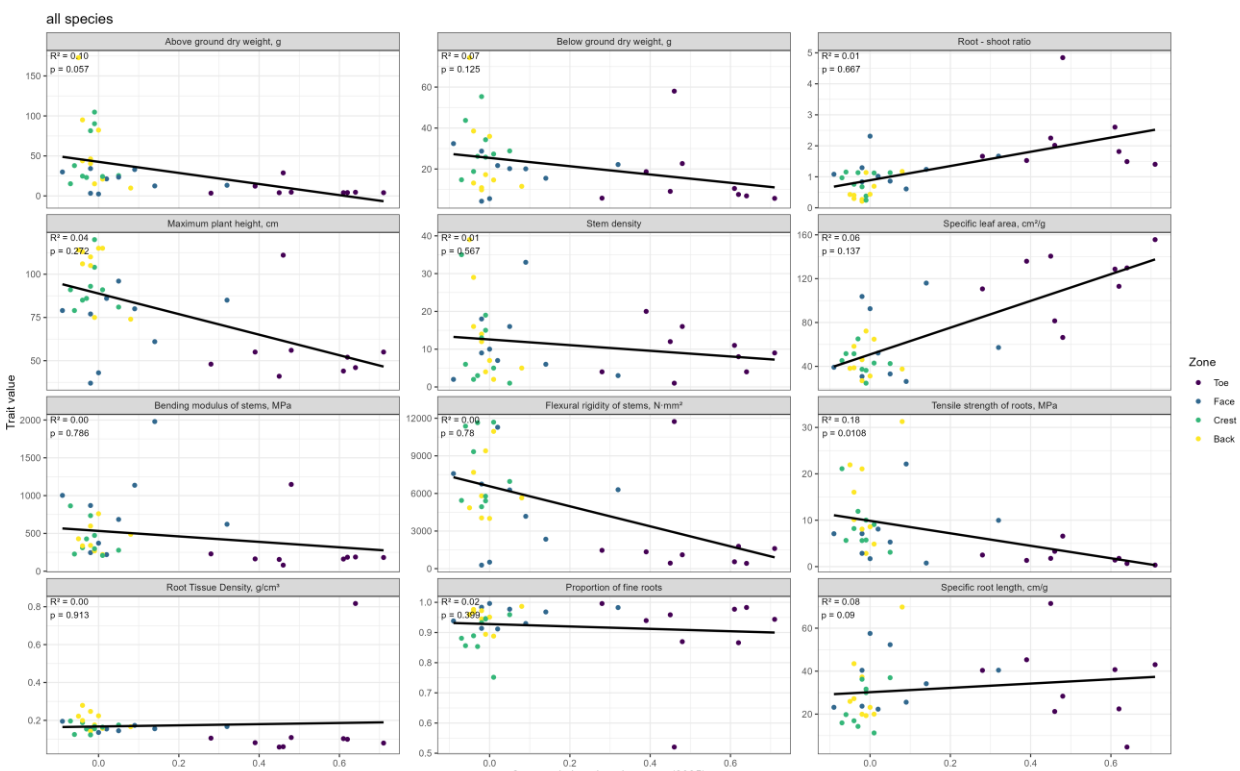

Figure 21: Trait variation of A. arenaria, E. farctus and L. arenarius with seasonal elevation change (March – September 2025).

The difference between consecutive DEMs indicated that the largest elevation changes occurred between May and July (Figure 22), following the establishment of a new foredune vegetation belt in March (Figure 23). Overlaying the elevation change from March to September with the vegetation distribution in July (NDVI values) reveals that the highest sediment accumulation occurred predominantly landward of the newly formed foredune vegetation belt, while strong erosion took place mainly in unvegetated areas (Figure 24).

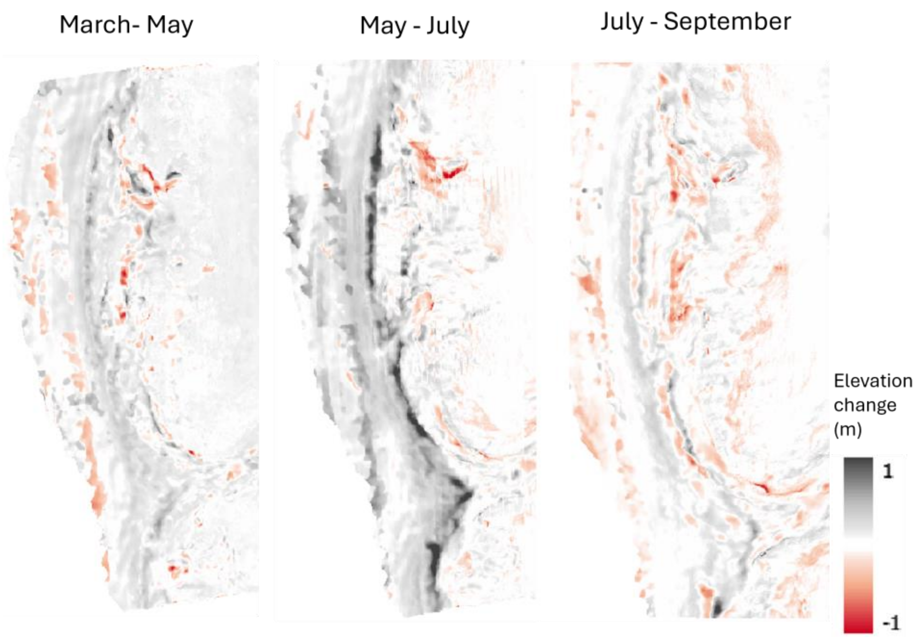

Figure 22: Elevation change or each measurement interval

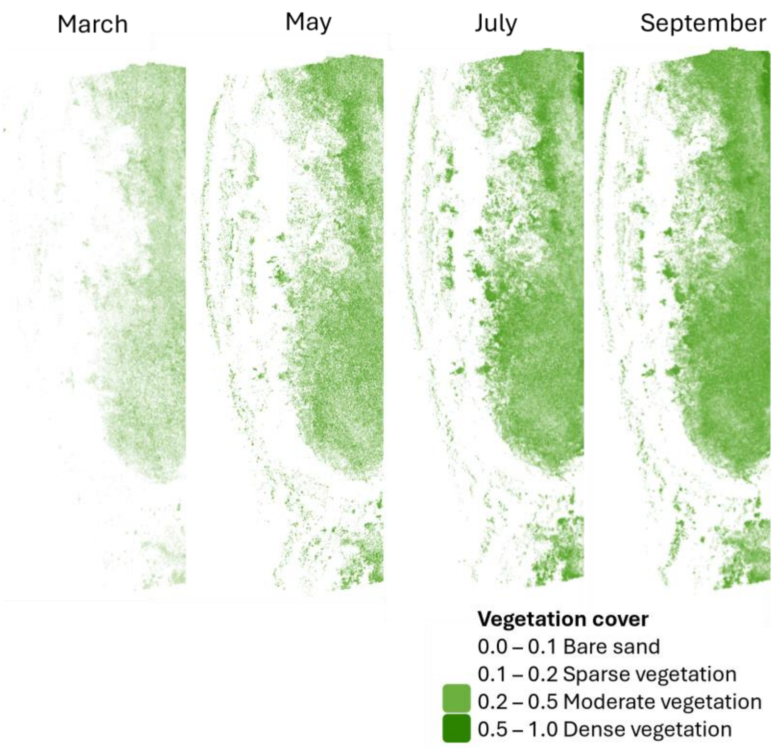

Figure 23: Vegetation coverage at each measurement date

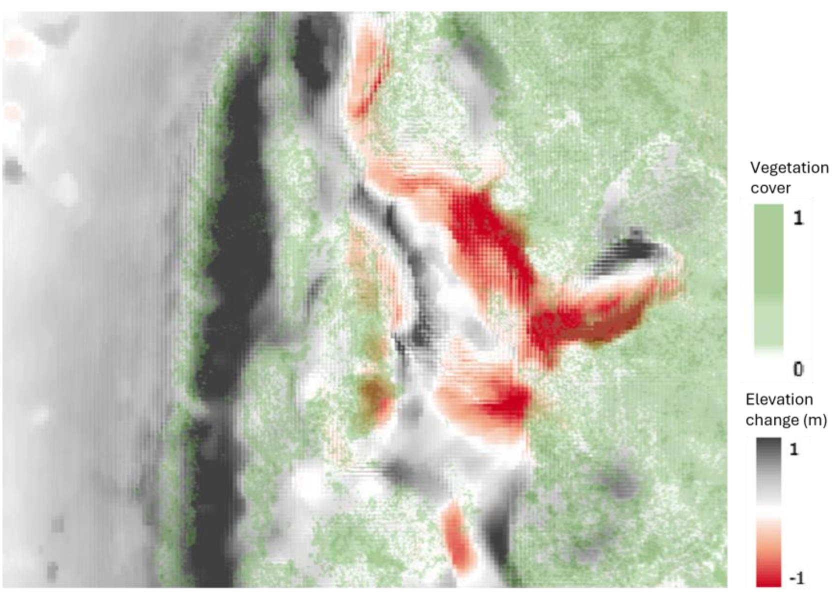

Figure 24: Total change in vegetation cover and elevation from March to September 2025.

As it is difficult to disentangle effect and response traits based solely on field observations, the experiments presented in the following chapter will allow a clearer separation of these mechanisms.

4. Plant effect traits

Coastal dunes serve as natural barriers that shield inland areas from wave impact, storm surges, and flooding. Their stability is strongly influenced by both above- and belowground vegetation, which alters sediment dynamics, enhances dune resilience, and reduces erosion during extreme events. Aboveground structures such as leaves and stems dissipate wave and wind energy by increasing surface roughness, slowing flow, and trapping sand, thereby limiting sediment loss and promoting dune growth. Belowground roots and rhizomes bind sand particles, strengthening the substrate and stabilizing sediments against erosion. These effects of dune vegetation have been well documented in previous studies (e.g., Feagin et al., 2019; Figlus et al., 2022), which provide a basis for linking the plant traits measured in Task 10.1 to effects on sedimentation, erosion resistance, and overall dune stability using both wave and wind physical experiment. However, previous wave flume experiments often fail to account for natural dune development. Because natural dunes evolve through successive burial events, we not only tested vegetation planted on the surface ("top-planted") but also replicated natural burial processes by gradually covering plants with sand ("bottom planted"). Using this approach, we conducted novel wave flume experiments with and at the Leichtweiß-Institute for Hydraulic Engineering and Water Resources, Technical University of Braunschweig, to relate measurable above- and below-ground plant traits to sand accretion and erosion potential (D10.1). Additionally, while previous wind tunnel experiments have been conducted to measure the effects of different plant traits (e.g., shoot density, shoot height) on sediment trapping using large scale wind tunnel facilities (6m l x 1m w x 2m h), the effects of vegetation on aeolian transport fluxes have not been quantified on small (single plant) scale dimensions.

4.1 Wave flume experiment with A. arenaria

To simulate realistic coastal dune systems under controlled conditions, vegetated dunes were first cultivated outside the laboratory in large crates. At the beginning of each erosion experiment, these crates were carefully transferred into the wave flume, ensuring that plant–sediment interactions develop under consistent and repeatable hydrodynamic forcing. The experiments are carried out in two phases. In the beginning of 2026 (Phase 1, the focus of this section), dunes with younger vegetation were tested to capture the early effects of plant establishment on erosion dynamics. After the submission of this Deliverable D10.1, a second series of experiments (Phase 2) will follow, focusing on more mature vegetation with more developed above- and belowground traits. This two-phase design allows the project to examine how plant age and growth stage influence dune stabilization.

4.1.1 Methods

Three dune configurations were compared. The first consisted of a dune with *A. arenaria* planted on the surface ("top-planted") at a density of 6 plants per square meter. The second mimicked natural burial processes, with the same density of plants incrementally covered by sand at a rate of 5 cm per month ("buried") (Figure 25). The third served as a control, consisting of an unvegetated dune. The *A. arenaria* plants were planted in October 2025. Each configuration was tested under identical hydrodynamic forcing.

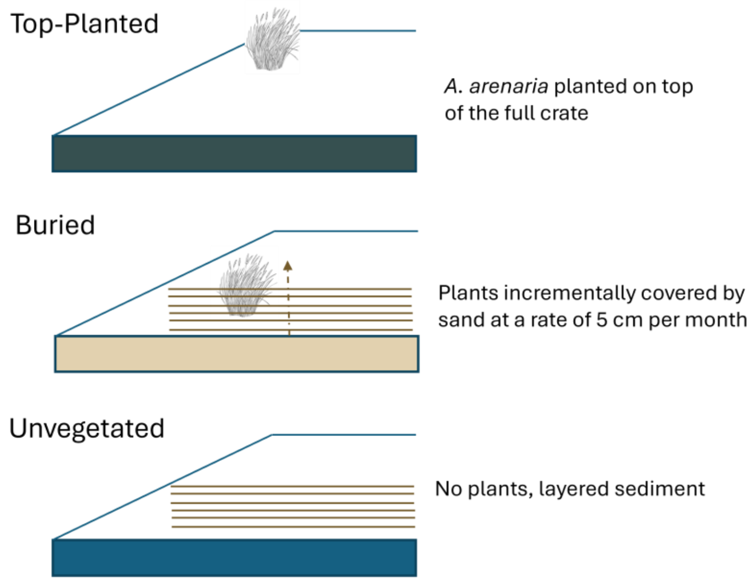

Figure 25: The three configurations used in the wave flume to study the effect of vegetation on wave run-up, overtopping, and reflection in coastal dunes.

Before each test, we measured some above ground plant traits like **number of stems** and **maximum plant height** of each individual. Other traits such as **above- and belowground biomass**, and **specific root length** and **root tissue density** were measured in the laboratory after the tests to capture both their structural and functional contributions to dune stability.

The crates where exposed to storm conditions that represent an extreme event with a 200-year return period under present-day conditions for St. Peter Ording. The experiments were conducted under a constant water level of 66 cm, with a significant wave height of 20 cm and a peak wave period of 3.3 seconds. Wave forcing was applied in a series of discrete bursts of increasing duration to simulate progressive storm impact. The first wave burst lasted 12 minutes, followed by subsequent bursts of 25, 35, and 63 minutes, respectively. This stepwise approach allowed the assessment of cumulative erosion and vegetation response under sustained hydrodynamic forcing (Figure 26).

Figure 26: Dune crate containing plants from the burial treatment before (left) and during the wave flume tests (right).

During the experiments, hydrodynamic, morphological, and sediment transport processes were monitored using a coordinated set of instruments (Figure 27). Ultrasonic wave gauges and pressure transducers recorded wave characteristics and dynamics across the beach, while Acoustic Doppler Velocimeters (ADV) measured flow velocities in three dimensions. Sediment transport and turbidity were quantified using Optical Backscatter Sensors (OBS).

Morphological changes were captured through LiDAR-based measurements of the above-water dune profile, complemented by pre- and post-experiment laser scanning. In addition, a trolley equipped with echosounders tracked profile development after each wave burst, and a camera system provided continuous visual documentation.

These measurements enabled the quantification of erosion and accretion processes through metrics such as sediment loss, volumetric change, and shifts in dune morphology, providing direct indicators of dune resistance under wave forcing.

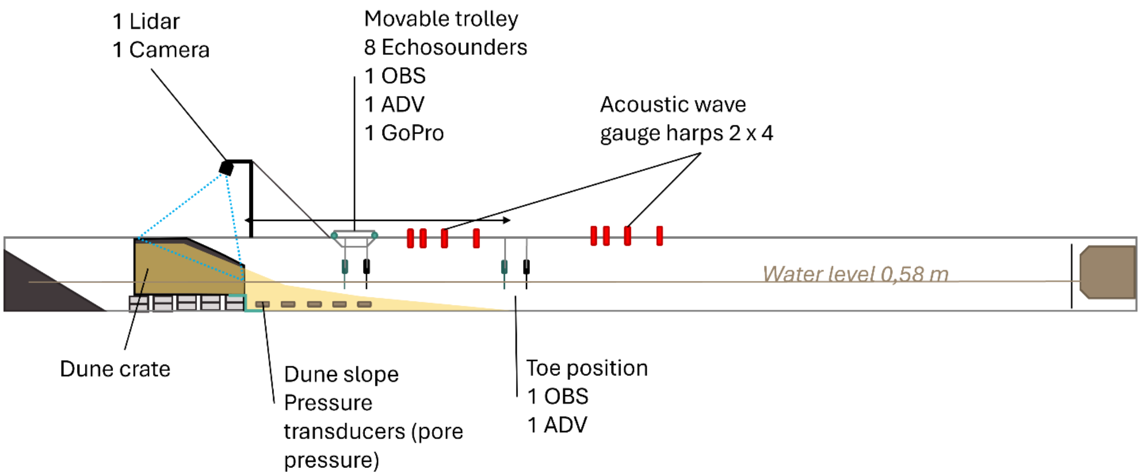

Figure 27: Setup of the wave flume with positioning of the dune crate and all applied sensors (by Oliver Lojek).

4.1.2 Results

The two treatments showed that burial has a strong influence on plant growth. In the buried treatment, plants exhibited significantly greater **stem density**, **specific root length** and **total dry biomass** compared to those in the top-planted treatment (Figure 28). Conversely, **root tissue density**, **maximum plant height**, and **stem diameter** were significantly lower under burial conditions.

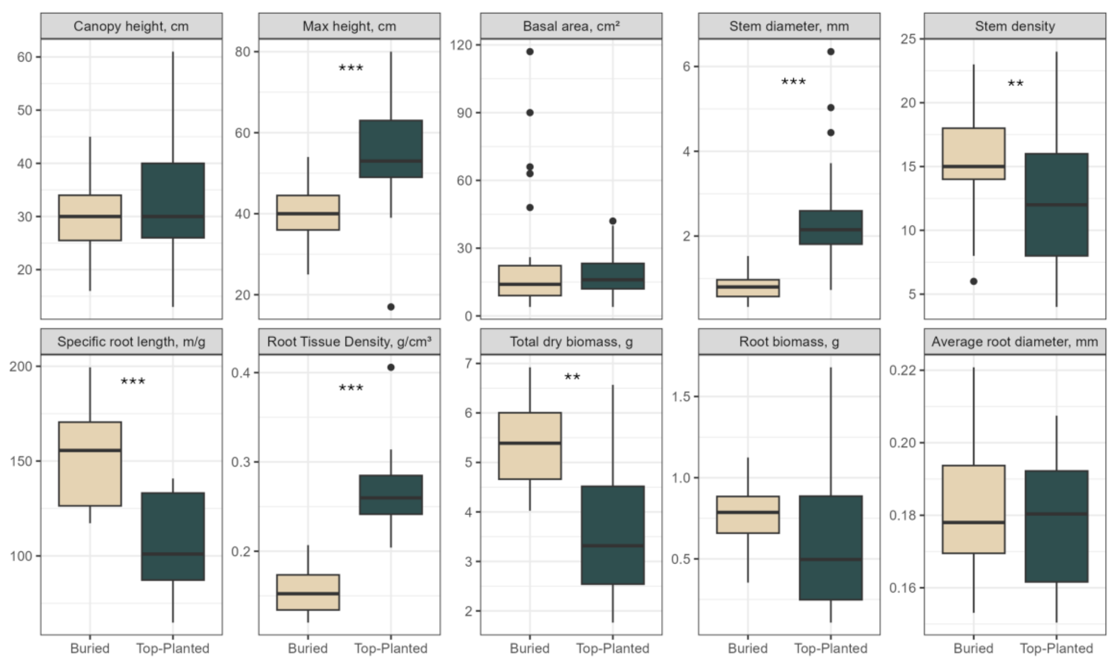

Figure 28: Above-and belowground plant traits of A. arenaria for the top-planted and burial treatments. Stars *indicate the results of Wilcoxon rank-sum tests (* : $p \leq 0.05$, ** : $p \leq 0.01$, *** : $p \leq 0.001$).*

The test in the wave flume showed that vegetation in general substantially slowed erosion processes (see D 12.2 for more details). Unvegetated dunes exhibited the same degree of erosion after the first wave burst that the vegetated dunes reached only after the third. Dunes with buried plants even remained intact until the fourth wave burst.

Planting treatment strongly influenced dune stability and plant dislodgement (Figure 29). The plants exposed to burial persisted throughout the experiment, with only one individual dislodged during the final wave burst. In contrast, top-planted individuals were rapidly washed out upon water contact, with six of 13 plants dislodged, including three during the first wave burst.

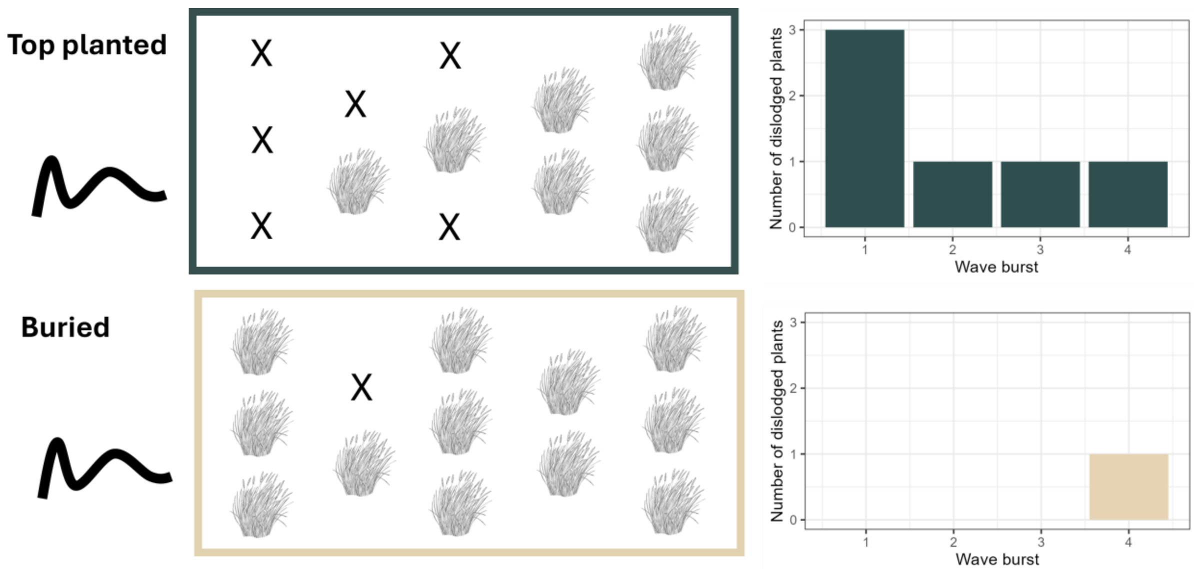

Figure 29: Spatial position (left) and timing (right) of plant dislodgement during the wave flume experiment, shown by treatment type.

4.2 Wind tunnel experiment

We developed a small-scale (1 m long, 20 cm wide and 40 cm high) portable wind tunnel, powered by two leaf blower systems. At the time of the deliverable (D10.1) the applicability of the portable wind tunnel was first tested in experimental conditions where we manipulated the sediment grain size composition, the presence of an armoured shell layer and the placement, density and number of dune grass individuals. All these factors were manipulated to assess to what extent a small-scale wind tunnel can be used to understand aeolian-mediated sediment transport processes in presence and absence of vegetation. Finally, we simulated all vegetation scenarios in the commonly used dune morphodynamic AeoLis model.

We applied two different vegetation-sedimentation modelling approaches to assess to what extent the wind tunnel can be used to calibrate existing (Aeolis) and novel (see deliverable 10.2 for the newly developed LivingDunes model) models. In the next phases (after the D10.1 deadline) we will further test the wind tunnel in the field using a selection of different dune engineering species measured in section 4.1 (e.g. *Ammophila arenaria*, *Elymus farctus, Cakile maritima, Leymus arenarius)* and by mimicking different trait combinations (derived from task 10.1) using plant mimics and 3D printing techniques.

4.2.1 Methods

Wind tunnel construction

For the DuneFront project a novel portable wind tunnel system was developed (Figure 30). The wind tunnel consists of four different modules that can be individually transported and assembled in the field. The first module consists of the wind generator, which is currently executed by two backpack leafblowers (ECHO PB-8010). The second module, the transformer box, consists of a pressure box, filters and a subsequent series of filters to transform the strong turbulent inflow of air to a stable controlled (unidirectional) wind flow. In the simulation chamber the wind flow remains confined to a cross-sectional area of 0.08 m2 (0.2 width, 0.4 height) over a one-meter long fetch. In this simulation chamber, the shear stress generated by wind flow – if above the required threshold – initiates movement in the sand particles, causing aeolian transport through creep, reptation, saltation and suspension.

The simulation chamber has one transparent side to allow for visual inspection and measurements during an experimental run. Additionally, the flume consists of several Structure for Motion (SfM) reference markers to analyse bed level changes by comparing Digital Elevation Models at the start and end of an experimental run (DoD). Finally, through holes in the roof an anemometer (Voltcraft PL-135HAN windmeter) can be inserted to measure the wind field during experimental runs (see Figure 31 for example). The fourth module at the end of the tunnel is the sediment collector. For this we used a bed sheet attached to a wooden frame that can be attached to the simulation chamber. Due to the porosity of the sheet, the moving air can freely escape, limiting the counter pressure inside the system, while most sediment particles are captured inside the sheet.

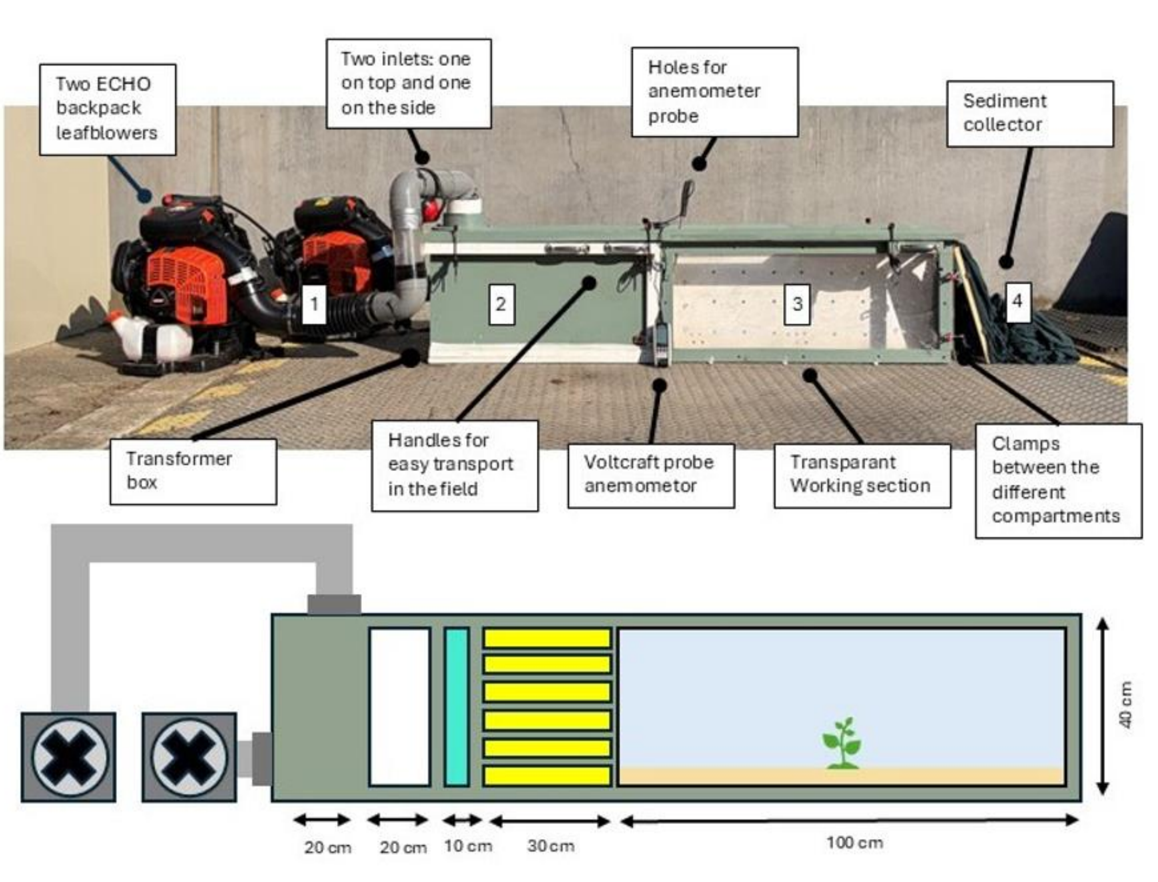

Figure 30: Photograph (top) and schematic overview (below) of the novel portable wind tunnel system that was specifically developed for the DuneFront project. The numbers in the top photo indicate the four (easily disassembled) modules which together make the wind tunnel: wind generator (1), wind transformer (2), simulation chamber (3) and sediment collector (4).

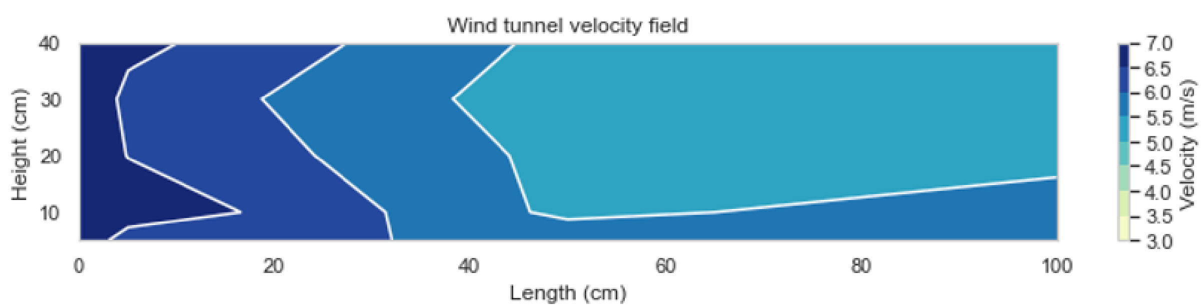

Figure 31: Wind tunnel velocity field based on measurements during experimental runs with on x-axis the length of the working section and on the y-axis the height. Wind speeds were, as expected, highest near the source and tend to increase slightly towards the bed. Overall, relatively constant wind speeds were observed.

Testing the applicability of the wind tunnel

We first conducted a series of experimental runs to assess the wind tunnel applicability and to determine to what error margins transport experiments are repeatable using well-sorted fine-grained sand (0.1-0.3 mm, bulk density 1513.9 kg/m^3). For this we first measured sediment transport using the collector module at regular time intervals to characterize the baseline transport rate and the measurement error. Figure 32 A shows a baseline transport rate of 0.1 dm^3 with a standard deviation of 0.069 dm^3 with an increase in fluctuation of 0.008 dm^3/min. While the exact transport rate depends on the used sediment, the standard deviation and run-time dependent increase is relatively small showcasing the repeatability of the flume and applicability for comparing different experimental simulations. In later experiments we chose 16-minute simulations.

We further tested three different sediment transport calculation methods: Structure for Motion (SfM) using a Nikon D5300 DLSR camera, as well as SfM using a standard phone lens (Motorola moto g14) and the weighing of the sediment collected in the collection module. The SfM method with the D5300 lens exhibits a compact volumetric error distribution centered around zero while both the phone lens and the collection module slightly underestimated sediment transport. The accuracy offset was smallest for the D5300 camera (0.027 dm3) compared to the phone lense (-0.069 dm3) and physical retrieval (-0.105 dm3), with measurement errors showing the same increasing order of 0.049, 0.05 and 0.128 dm3. This shows that the SfM method errors are smaller than the flume fluctuations, while the sediment collector module's error is slightly larger (Figure 32 B). This is probably explained by both sediment losses during simulation (the sheet porosity does not prevent the smallest particles from escaping) and introduced measurement errors by collecting sediment from the sheet and weighing errors. However, it should be noted that the processing time for the SfM method is much higher due to high resolution image capturing (±300 images taking 5-9 minutes) and processing time from raw images to DEM using python MetaShape scripts (10-15 minutes per run).

For these reasons for the vegetation experiments we choose to calculate the transport rate by weighing the residual sediment in the simulation chamber (to overcome problems related to sediment and run time) and use this as the response variable in all experimental runs.

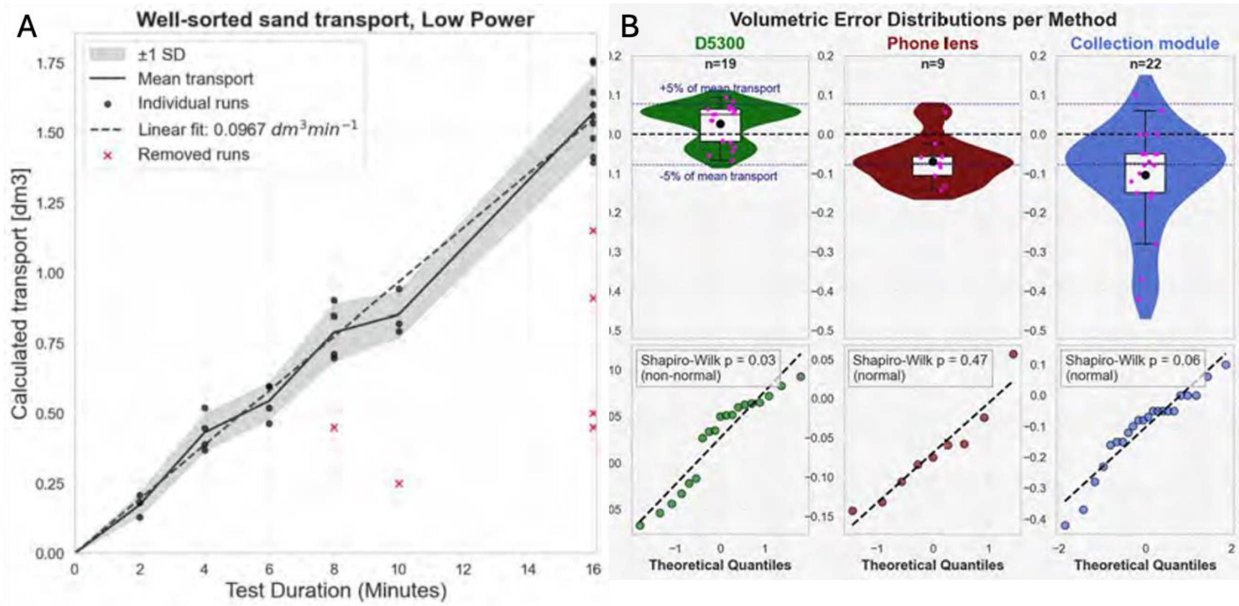

Figure 32: Test run results showing A) the baseline transport in dm³ with a well-sorted sediment mixture (0.1-0.3 mm) during a wind velocity of approximately 7 m s-1. Red crosses indicate erroneous runs that were omitted due to cold-start of leaf blowers or leaking of air flow. B) showcases violin-box plots of absolute volumetric error per method (SfM Nikon D5300 lens, SfM phone lens and physical retrieval collector module), measured in comparison to the measured physical volume of sediment that remained in the simulation chamber following experimental runs.

Measuring vegetation-sedimentation processes in an experimental wind tunnel

Once we developed and validated the applicability of the wind tunnel (previous sections) we carried out a series of 20 different vegetation scenarios (Figure 33 for overview) to understand how vegetation affects sediment transport rates. Unfortunately, due to time constraints we were for now only able to derive an estimate of the importance of basic vegetation properties (density and patch size) using the same dune building species (*A. arenaria)* that was positioned in different sections of the flume (upwind, mid-fetch or downwind). As all experimental runs were performed in late March 2026 the plants were effectively still in winter dormancy. Furthermore, due to the limited dimensions of the flume we clipped off the aboveground biomass to fit within the 40 cm height simulation chamber. Finally, we were unable to perform experimental runs yet within the field (which requires multiple days without rain to prevent sediment moisture which effectively hampers transport). Therefore, we here only tested canopy effects leaving the effects of belowground material still unaccounted for. As a result, we attached all plant material to the test bed level designed for operating the flume in laboratory conditions. All experimental runs were performed using uniform fine-grained material (both sediment and plants were collected from Sand Engine, DuneFront demonstator Delflandse kust, Figure 1) and for a simulation time of 16 minutes.

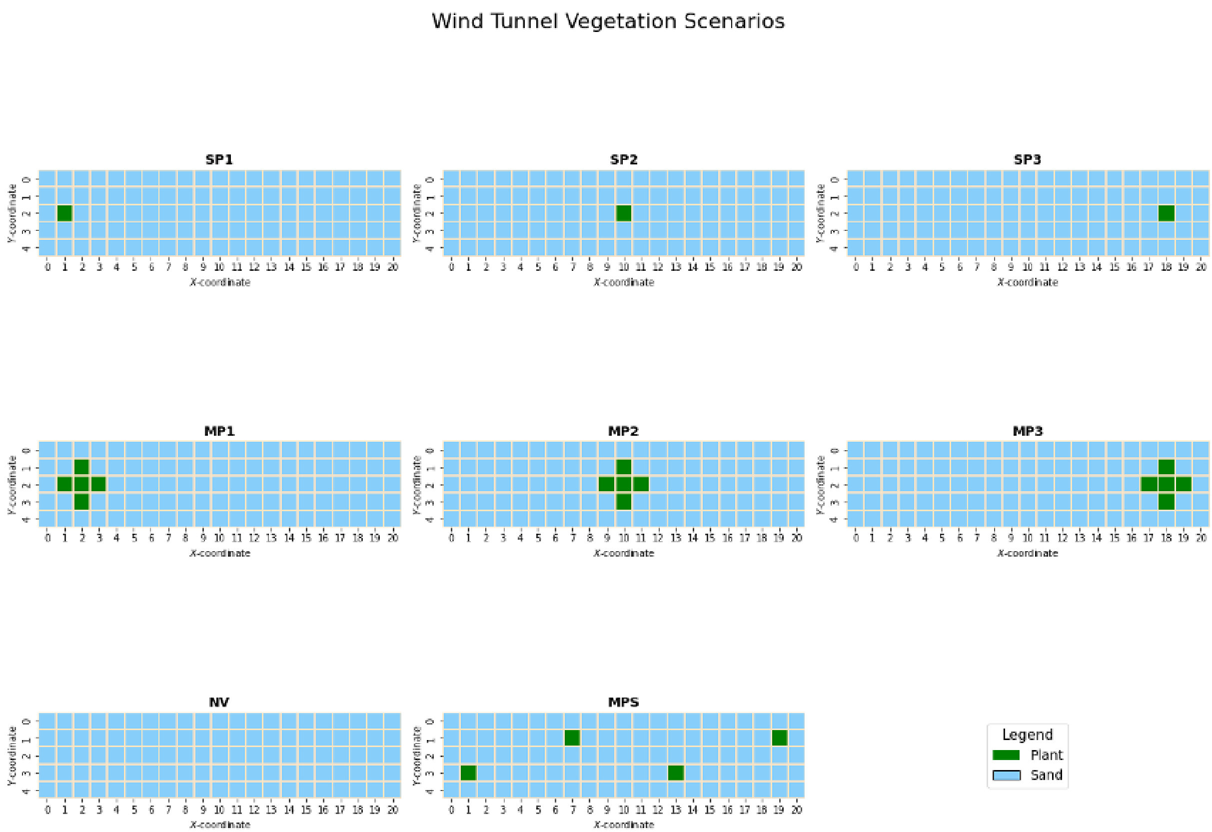

Figure 33: The different planting scenarios divided by small patch (SP top panels) consisting of a single plant, medium patch (MP) consisting of four closely spaced individuals. No vegetation scenario (NV bottom) and the dispersed plant scenario (bottom right MP). Furthermore, the single (SP) and multiple (MP) patch scenarios were executed with the plant material at three separate sections of the flume. Furthermore, we tested all SP and MP scenarios for 2 different densities with each plant either consisting of ~6 (low density), ~20 (medium density) or ~41 stems (high density).

For the result interpretation we analysed the normalized transport rate which was calculated by comparing the transported sediment of a certain vegetation treatment (kg) with the no vegetation control treatment (which was on average 0.75 kg during the 16-minute runtime). We found that for the single-plant configurations vegetation position had a significant effect (p=0.003) on sediment transport with increased transport upwind and near zero to decreasing transport rates in mid fetch or downwind. While vegetation density had only a significant effect upwind (2.5 times higher than the unvegetated control, Figure 34), in the mid-fetch position we did observe a slight reduction while downwind the effect seems negligible. For the multiple plant scenarios, we observed more complex effects with both density and position significantly affecting sediment transport (Figure 35). Here, the higher density (upwind and downwind position) or even the medium density (downwind) had a negative effect on sediment transport, leading to accelerated flow and erosion. In contrast the low density led to reduced erosion at al positions with the medium density showing contrasting outcomes depending on the position. Due to time constraints, we did not apply the SfM method here to provide a local analysis op bed level changes but based on our observation we can provide an explanation for the observed effects.

The transport increases were clearly the result of funnelling or accelerated flow effects around vegetation patches (Figure 36) that were observed and measured around (large or dense) vegetation patches. The effects are strongest for high density patches containing multiple plants that are positioned upwind (with normalized transport of 231% and 290% for single and multiple plants, respectively). They are positioned close to the wind source and due to the dimensions of the wind tunnel (closed top) wind cannot pass through the stems resulting in strong funnelling around the plants (Leenders et al. 2021, Duan et al. 2024). In beach environments the wind would of course escape in the vertical dimension which also makes the transport medium of wind so contrasting to water and water flow driven transport in flow or tide-dominated wetlands. In contrast the reduction of total sediment transport by the other configurations is caused by sediment trapping of the vegetation in the wake. In the downward position this effect was hindered as all sediment was trapped in the collector module and therefore accounted for as eroded (Figure 37).

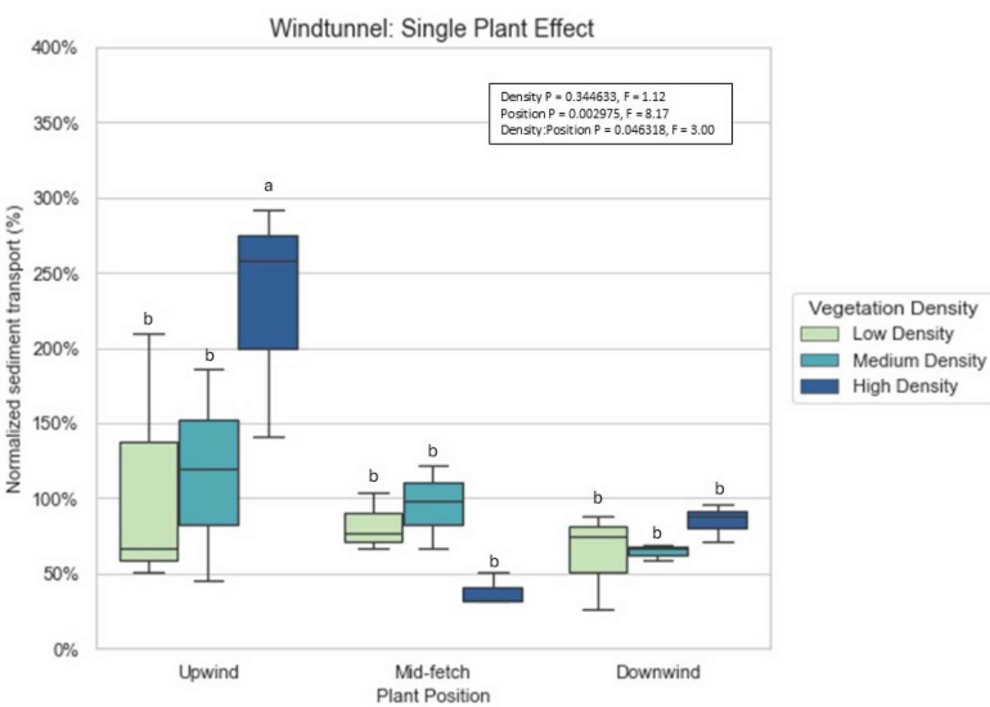

Figure24: Results from the wind tunnel experiment for the single (small) plant configurations. Vegetation position has a large effect on sediment transport, while density only mattered for the plants in the upwind section.

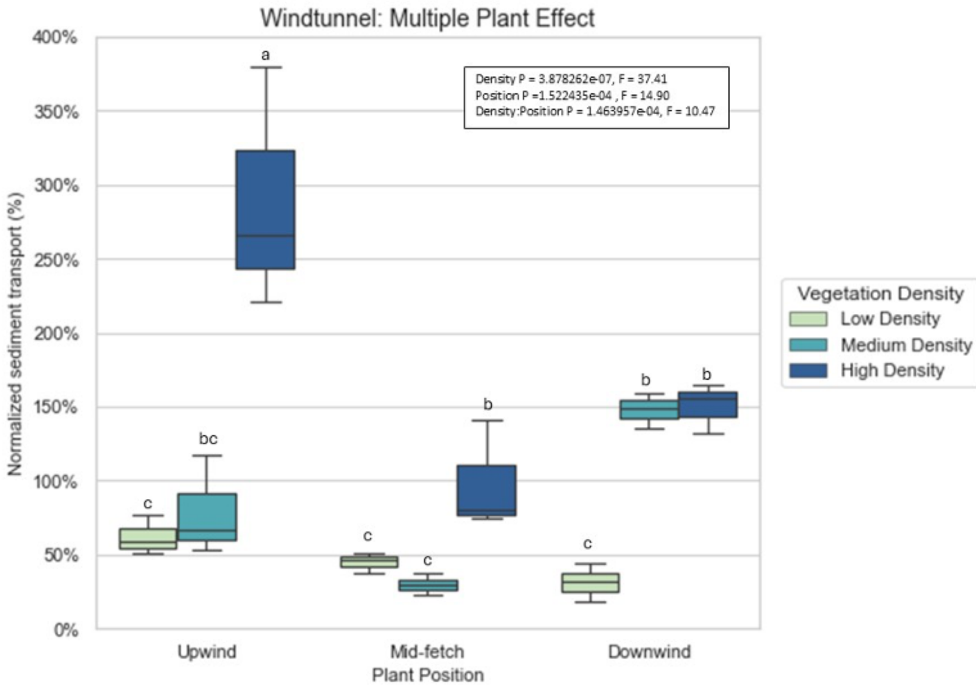

Figure 35: Results from the wind tunnel experiment for the multiple (medium) plant configurations. Both vegetation position and density can significantly affect sediment transport. In general, high density leads to increased transport (compared to unvegetated control), while transport reduction was observed for all low-density configurations.

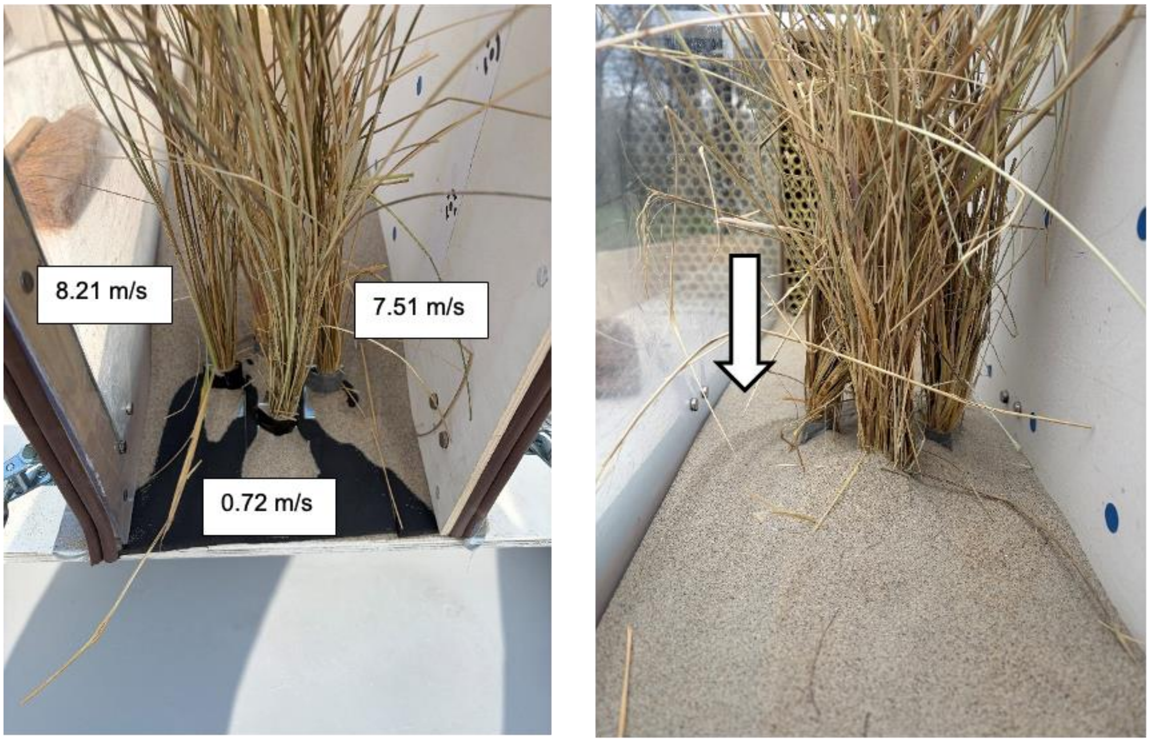

Figure 25: left image: accelerated wind speeds were observed at sides of the vegetation (from 6 m/s in front of plant to ~8 m/s adjacent to plant while a significant decrease was measured in the wake. Right image shows a channel directly adjacent to the plant with visible higher sediment transport due to accelerated wind speeds while in the plant's wake no sediment mobility was observed.

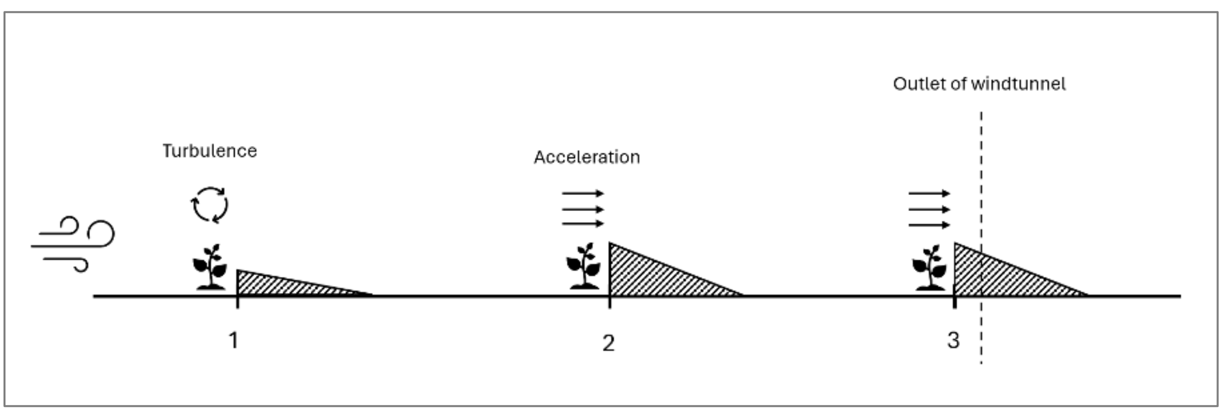

Figure 26: Schematic representation of processes happening inside the wind tunnel illustrating the relationship between localized flow acceleration, sediment trapping mechanisms, and the resulting sediment transport. At an upwind position (1) the vegetation exerts major turbulence, resulting in significant flow accelerations and an increase in sediment transport. Mid-fetch (2) seems to be the ''sweet spot'' where the most sedimentation occurred. Downwind (3) we observe a false quantity of sediment transport because of the cut-off deposition wake due to the outlet of the wind tunnel.

4.2.2 Results

The findings from the wind tunnel experiments indicate that vegetation exerts a dual influence on sediment transport. While plants facilitate deposition by trapping suspended sediment in their lee, they also increase transport by diverting airflow and increasing local wind velocities. These outcomes are primarily controlled by vegetation spatial configuration and density but should be interpreted with caution as they are also dependent on the spatial dimensions of the wind tunnel that prevent vertical funnelling of the wind, over the vegetation canopy. This phenomenon has been observed during storm conditions in coastal dunes as well and can lead to accelerated skimming wind flow over vegetated patches (Rotnicka et al. 2023).

In the current set-up, we applied a constant wind flow but for future tests it would be interesting to see how the vegetation interacts with the in-flume wind field and affects sediment transport rates and shear stress thresholds over progressively increasing wind speeds. Additionally, while the flume set-up affects the vertical flow field it does yield interesting results regarding the effects of vegetation traits on wind flow modulation and sedimentation processes. In the future we wish to further test the impact of differences in trait expression using living plant material (including different species and 3D-printed mimics) and use the findings to calibrate existing or novel (see D10.2) process-based numerical models that simulate dune morphodynamics.

As a first step we calibrated the process-based AeoLis model (van Wetsel et al., 2024) to simulate the small spatial dimension of our flume and using both the Okin and Raupach vegetation-sedimentation solver. The Okin solver interpolates the wake influence over longer distance (kernel) than the often-used Raupach method which only looks at close neighbouring cells. We found that in the AeoLis model vegetation density currently had no effect, but position had, with a progressive declining effect for Okin with increasing distance from the wind source, while the Raupach method showed the opposite trend (Figure 38). As the Okin method simulated the wake effect the limited dimension of the wind flume cut off the sediment capturing effect in the wake, similar to the physical experiments using our wave flume for the multiple plant scenarios (Figure 37 and 39).

These preliminary modelling results show that the vegetation solvers provide very contrasting results with minimum effects of vegetation for the Raupach (0 to 27% sedimentation reduction) while the Okin solver completely reduced sediment transport when the plants were planted close to the source. Furthermore, the absence of a vegetation density effect shows that parametrization of local vegetation density can be improved further. We conclude that while both the physical experiments and model simulations still show flaws, they are promising and labour and cost-effective methods to simulate and study physical small-scale processes. Furthermore, executing physical experiments and model simulations in parallel helps gain more system understanding and can be directly translated to (adjusted or parameterized model equations). This can then be used to inform decisions on Dune-dike hybrid constructions on for instance sediment source material and application and vegetation planting strategies.

Figure 27: AeoLis model results for the simulated plant scenarios with different positions, shoot densities and plant numbers normalized to the bare (no vegetation) scenario. The Top plots indicate the results from Raupach, while the bottom panels indicate the Okin results.

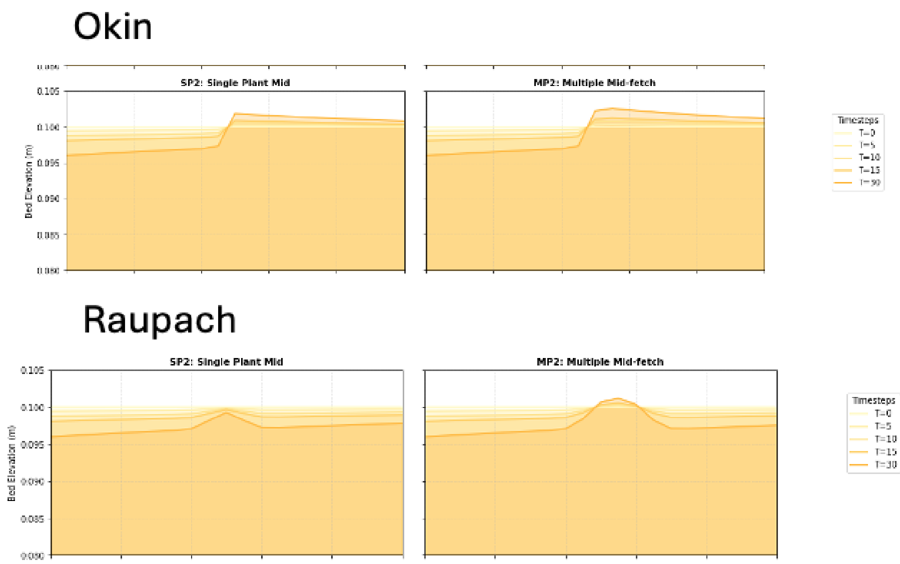

Figure 28: Bed level evolution for single and multiple plant scenarios at the mid-fetch position for both Okin (top) and Raupach (bottom).

5. Conclusion

This report evaluates key dune species using a trait-based approach to quantify vegetation-sediment interactions. A multi-method approach combining field sampling, remote sensing and laboratory experiments, was applied to clarify the complex interactions that underpin functionality of vegetated dunes.

Our study addresses key research gaps through comprehensive field data collection that includes both above- and belowground traits across multiple species and investigates regional differences across Europe.

We demonstrated substantial variability in plant response traits, with clear evidence of both interspecific and intraspecific trait variation. Pronounced interspecific differences were observed in above- and belowground traits; for example, grass species showed the highest and most variable specific root length and the lowest specific leaf area compared to the other species. Intraspecific variation was also evident, as shown by comparisons across all study sites, with *E. fractus* exhibiting greater variability than *A. arenaria*.

Analysing vegetation-sediment feedback at multiple spatial and temporal scales, we found that sediment accretion conditions induced some trait adjustments, including increased root–shoot ratio, plant height, specific root length, and the proportion of fine roots, indicating enhanced belowground investment and overall growth in response to sediment accumulation. Multi-year monitoring of *A. arenaria* plantings showed a positive relationship between vegetation cover and both sand deposition and dune growth. The strongest effects were observed during the first two years, while the second and third years exhibited a more stabilized pattern of sustained positive dune development. Linking functional traits to dune dynamics in St. Peter Ording revealed systematic variation in trait expression across stress zones, with the strongest differences observed in the highly dynamic toe area. However, only root tensile strength showed a significant decrease with increasing elevation change during the growing season. Spatial patterns of erosion and deposition highlight a strong vegetation effect on dune development: Sediment accumulation was concentrated landward of the developing foredune vegetation belt, while erosion predominantly occurred in unvegetated areas, underscoring the role of vegetation in stabilizing and shaping dune morphology.

While our field research provides quantitative, mechanistic insights into vegetation–sediment interactions and expands trait datasets for dune species—particularly for previously underrepresented belowground traits relevant to sediment stabilization—the complex relationships between plant characteristics (e.g., stem flexibility, shoot structure, height, and root traits) and erosion and accretion processes required disentangling through carefully designed and controlled experiments.

A wave flume experiment provided important insights into the effects of sedimentation. Burial strongly influenced plant growth, affecting both above- and belowground traits. As a consequence, the sedimentation regime had a pronounced impact on the ability of plants to remain intact and anchored during simulated storm events and, in turn, to support dune stability. However, the data presented from the wave flume experiments in this report are not yet complete and will be complemented by Deliverable 12.2. Additional experiments with longer growth periods and alternative planting schemes are planned and are expected to provide further insight into the processes governing vegetation–sediment interactions and dune development.

Within this report, we also presented a prototype of a portable wind tunnel. The development of this new device addresses challenges associated with logistics in using large experimental wind tunnels. It enables a wide range of possible experiments and adaptability allowing for further testing of plant effects on wind flow and sediment transport and deposition. The portability of this device enables in-field testing on real plants significantly improving the data quality gained from related experiments which will greatly enhance our understanding of the vegetation-sediment feedback processes which drive dune development. These findings provide promising results which will be integrated into the process-based model LivingDunes and feed Deliverable 10.2.

In summary, our findings improve the understanding of how vegetation–sediment interactions are governed by plant functional traits and demonstrate their importance for dune formation, stability, and resistance to erosion under dynamic coastal conditions:

We found that plant height, stem density, specific root length, root surface area, and root tensile strength ***respond*** to burial. Plant height, stem density, and aboveground biomass ***affect*** sand trapping where belowground biomass, root tissue density and root tensile strength ***affect*** sediment stability.

This report lays a groundwork for future research to further untangle the complex relationships between plant growth and dune stability and ultimately enable improved planning of NbS. The trait–process relationships established in this study provide an empirical basis for improving and parameterizing the process-based model “Living Dunes”, enabling more accurate predictions of coupled vegetation–sediment dynamics across spatial scales. Overall, integrating trait-based ecology with modelling will allow for scenario-based assessments of current and future dune-building capacity. The resulting predictive framework will provide evidence-based guidance for coastal management, climate adaptation, and biodiversity-inclusive Nature-based Solutions.

6. References

Adeli A., Gruwez V., Troch P., Hofland B., Tissier M., Bonte D. (2024). Comprehensive investigation of existing designs of the DuneFront Demonstrators, Version 1.0, DuneFront Project Deliverable 7.1, Ghent University.

Castelle, B. ; Dahirel, M. (2024). DuneFront: Deliverable 4.1 - Physical boundary counditions. Version 1.0. Université de Bordeaux : Bordeaux. 30 pp.

Ciccarelli, Daniela; Bona, Cleusa (2022): Exploring the Functional Strategies Adopted by Coastal Plants Along an Ecological Gradient Using Morpho-functional Traits. In Estuaries and Coasts 45 (1), pp. 114–129. DOI: 10.1007/s12237-021-00945-y.

Dahirel, M. and Bonte, D. (2025). Biological boundary conditions, version 1.0, DuneFront project deliverable 4.2, Ghent University.

Feagin, R. A.; Furman, M.; Salgado, K.; Martinez, M. L.; Innocenti, R. A.; Eubanks, K. et al. (2019): The role of beach and sand dune vegetation in mediating wave run up erosion. In Estuarine, Coastal and Shelf Science 219, pp. 97–106. DOI: 10.1016/j.ecss.2019.01.018.

Figlus, Jens; Sigren, Jacob M.; Feagin, Rusty A.; Armitage, Anna R. (2022): The Unique Ability of Fine Roots to Reduce Vegetated Coastal Dune Erosion During Wave Collision. In Front. Built Environ. 8, Article 904837. DOI: 10.3389/fbuil.2022.904837.

Freschet, Grégoire T.; Roumet, Catherine; Comas, Louise H.; Weemstra, Monique; Bengough, A. Glyn; Rewald, Boris et al. (2021): Root traits as drivers of plant and ecosystem functioning: current understanding, pitfalls and future research needs. In The New phytologist 232 (3), pp. 1123–1158. DOI: 10.1111/nph.17072.

Lavorel, S.; Garnier, E. (2002): Predicting changes in community composition and ecosystem functioning from plant traits: revisiting the Holy Grail. In Functional Ecology 16 (5), pp. 545–556. DOI: 10.1046/j.1365-2435.2002.00664.x.

Lavorel, Sandra (2013): Plant functional effects on ecosystem services. In Journal of Ecology 101 (1), pp. 4–8. DOI: 10.1111/1365-2745.12031.

Leenders, J. K., Sterk, G., & Van Boxel, J. H. (2011). Modelling wind-blown sediment transport around single vegetation elements. Earth Surface Processes and Landforms, 36(9), 1218–1229. https://doi.org/10.1002/esp.2147

Lowe, E.B., Iuliano, B., Gratton, C. et al. 'Scalescape': an R package for estimating distance-weighted landscape effects on an environmental response. Landsc Ecol 37, 1771–1785 (2022). https://doi.org/10.1007/s10980-022-01437-5

McGuirk, Marita T.; Kennedy, David M.; Konlechner, Teresa (2022): The Role of Vegetation in Incipient Dune and Foredune Development and Morphology: A Review. In Journal of Coastal Research 38 (2). DOI: 10.2112/JCOASTRES-D-21-00021.1.

Mordacq, O; Dahirel, M (2025). Habitat & vegetation evolution in Demonstrators, version 1.0, DuneFront project deliverable 5.1. University of Bordeaux, Ghent University.

Pérez-Harguindeguy, N.; Díaz, S.; Garnier, E.; Lavorel, S.; Poorter, H.; Jaureguiberry, P. et al. (2013): New handbook for standardised measurement of plant functional traits worldwide. In Aust. J. Bot. 61 (3), p. 167. DOI: 10.1071/BT12225.

Raupach, M. R. (1992). Drag and drag partition on rough surfaces. Boundary-Layer Meteorology, 60(4), 375–395.

Robin, N., Ruz, M-H., Castelle, B., Blaise, E., 2025. Morphodynamics patterns, DuneFront Project Deliverable 6.1, Ghent University.

Rotnicka, J., Dłużewski, M., Hesp, P. A. & Tomczak, J. O. Skimming Flow and Sand Transport Within and Above Ammophila (Marram) Grass on a Foredune. J Geophys Res Earth Surf 128, e2023JF007143 (2023).

Zarnetske, Phoebe L.; Hacker, Sally D.; Seabloom, Eric W.; Ruggiero, Peter; Killian, Jason R.; Maddux, Timothy B.; Cox, Daniel (2012): Biophysical feedback mediates effects of invasive grasses on coastal dune shape. In Ecology 93 (6), pp. 1439–1450. DOI: 10.1890/11-1112.1.